Exploring the Influence of Ancillary Ligand Charge and Geometry on the Properties of New Coordinatively Unsaturated Cp*(κ^2-*P*,*N*)Ru$^+$ Complexes: Linkage Isomerism, Double C−H Bond Activation, and Reversible α-Hydride Elimination

Matthew A. Rankin,[†] Robert McDonald,[‡] Michael J. Ferguson,[‡] and Mark Stradiotto*,[†]

Department of Chemistry, Dalhousie University, Halifax, Nova Scotia, Canada B3H 4J3, and X-Ray Crystallography Laboratory, Department of Chemistry, University of Alberta, Edmonton, Alberta, Canada T6G 2G2

Received June 27, 2005

The synthesis, characterization, and reactivity properties of new Cp*Ru complexes supported by κ^2-*P*,*N*-1-P^{i}Pr$_2$-2-NMe$_2$-indene (**1a**), κ^2-*P*,*N*-2-NMe$_2$-3-P^{i}Pr$_2$-indene (**1b**), and κ^2-*P*,*N*-2-NMe$_2$-3-P^{i}Pr$_2$-indenide (**1**) are described (Cp* = η^5-C$_5$Me$_5$). Addition of **1a** to (Cp*RuCl)$_4$ afforded Cp*Ru(Cl)(κ^2-*P*,*N*-**1a**) (**2a**, 92%), which in turn was transformed into Cp*Ru(Cl)(κ^2-*P*,*N*-**1b**) (**2b**, 85%). Treatment of either **2a** or **2b** with AgBF$_4$ in acetonitrile provided the corresponding 18-electron, base-stabilized cation [Cp*Ru(CH$_3$CN)(κ^2-*P*,*N*-**1a**,**b**)]$^+$BF$_4^-$ (**3a**, 89%; **3b**, 91%). In the pursuit of the analogous acetonitrile-free, 16-electron species (**4a** or **4b**), complexes **2a** or **2b** were treated with Li(Et$_2$O)$_{2.5}$B(C$_6$F$_5$)$_4$. In the case of **2a**, the linkage isomer [Cp*Ru(η^6-**1a**)]$^+$B(C$_6$F$_5$)$_4^-$ (*endo*-**4c**, 74%) was obtained; exposure of this complex to triethylamine afforded [Cp*Ru(η^6-**1b**)]$^+$B(C$_6$F$_5$)$_4^-$ (**4d**, 85%). In contrast, chloride abstraction from **2b** generated the C−H bond activation product **4e** (83%); variable-temperature NMR data revealed that the apparent cyclometalation of **4b** to give **4e** is reversible. While the base-stabilized zwitterion **5a**·CH$_3$CN was successfully prepared (83%), attempts to generate the coordinatively unsaturated zwitterion Cp*Ru(κ^2-*P*,*N*-**1**) (**5a**) instead resulted in the formation of the isomeric hydridocarbenes **5b** (80%) and **5c** (84%). The apparent rearrangement of **5a** to a hydridocarbene is noteworthy, as it represents a remarkably facile, ligand-assisted double geminal C−H bond activation process. Moreover, data obtained from 1D- and 2D-EXSY NMR experiments involving **5c** provided compelling evidence for what appears to be the first documented interconversion of Ru(H)═CH and Ru−CH$_2$ groups by way of reversible α-hydride elimination. In keeping with this dynamic process, treatment of **5c** with PHPh$_2$ afforded the alkylruthenium adduct **6** (70%). Single-crystal X-ray diffraction data are provided for **2a**, **2b**, **3a**, **3b**·1.5C$_5$H$_{12}$, **4d**, **4e**, (**5a**·CH$_3$CN)·0.5CH$_3$CN, **5c**, and **6**·0.5C$_5$H$_{12}$.

Introduction

The development of mild and selective processes for the conversion of hydrocarbons into "value-added" products represents an ongoing challenge that spans a range of traditional chemical disciplines.[1] Many of the recent breakthroughs that have been made in this regard have resulted from the investigation of coordinatively unsaturated platinum-group metal complexes; a growing number of such complexes have been identified that are capable of mediating the selective cleavage and functionalization of otherwise unactivated C−H bonds under relatively mild stoichiometric and/or catalytic reaction conditions.[2] Notwithstanding these noteworthy achievements, our understanding of the way in which supporting ligands influence C−H bond activation processes within a metal coordination sphere is still rather limited.[3] As a result, the synthesis and structural characterization of new classes of coordinatively unsaturated platinum-group metal complexes supported by a series of structurally related ancillary ligands is of considerable interest, since reactivity studies involving such complexes can help to shed light on the complicated relationship between ancillary ligand steric and electronic parameters and metal-mediated C−H bond activation behavior.

In light of the established ability of coordinatively unsaturated platinum-group metal cations to activate

* To whom correspondence should be addressed. Fax: 1-902-494-1310. Tel: 1-902-494-7190. E-mail: mark.stradiotto@dal.ca.
† Dalhousie University.
‡ University of Alberta.

(1) Labinger, J. A.; Bercaw, J. E. *Nature* **2002**, *417*, 507.

(2) (a) Shilov, A. E.; Shul'pin, G. B. *Chem. Rev.* **1997**, *97*, 2879. (b) Dyker, G. *Angew. Chem., Int. Ed.* **1999**, *38*, 1698. (c) Crabtree, R. H. *J. Organomet. Chem.* **2004**, *689*, 4083, and references therein.

(3) Mechanistic details of the rhodium-catalyzed functionalization of alkanes to give terminal alkylboronate esters have recently been reported: Hartwig, J. F.; Cook, K. S.; Hapke, M.; Incarvito, C. D.; Fan, Y.; Webster, C. E.; Hall, M. B. *J. Am. Chem. Soc.* **2005**, *127*, 2538.

10.1021/om050534e CCC: $30.25
Publication on Web 09/15/2005

Chart 1

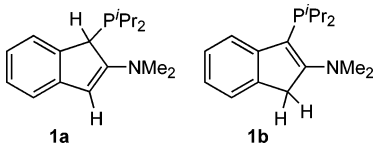

C−H bonds,[4] and given the improved reactivity characteristics commonly exhibited by κ^2-*P,N* complexes of this type relative to P,P or N,N species,[5] one aspect of our research focuses on the preparation of new coordinatively unsaturated platinum-group metal cationic complexes featuring κ^2-*P,N*-1-P^{i}Pr$_2$-2-NMe$_2$-indene (**1a**), κ^2-*P,N*-2-NMe$_2$-3-P^{i}Pr$_2$-indene (**1b**), and related ligands (Chart 1).[6] We are particularly interested in evaluating how geometric differences between **1a** and **1b** influence the stability, reactivity, and other properties of the associated complexes. We are also targeting structurally related zwitterions supported by κ^2-*P,N*-2-NMe$_2$-3-P^{i}Pr$_2$-indenide (**1**), which feature a formally cationic metal fragment counterbalanced by a sequestered, uncoordinated 10π-electron indenide unit built into the backbone of the P,N ligand.[6a] Our principal interest in developing unsaturated platinum-group metal zwitterions of this type for use in catalytic applications arises from the fact that such bidentate complexes often possess appealing reactivity characteristics commonly associated with more traditional cationic species, while at the same time exhibiting increased solubility in low-polarity media and heightened tolerance to coordinating solvents.[6a,7] Moreover, coordinatively unsaturated zwitterions supported by **1** also represent appealing candidates for the development of particularly challenging transformations involving the activation of multiple C−H bonds on one or more substrates;[8] the indenide fragment in this anionic ligand is poised to accept a proton from a formally cationic metal center following an initial C−H bond activation step, thus providing a means of re-establishing coordinative unsaturation at the reactive metal center and enabling subsequent C−H bond activation processes.

In the course of our investigations, we identified the coordinatively unsaturated 16-electron cations, Cp*Ru(κ^2-*P,N*-**1a**,**b**)$^+$, and the structurally analogous zwitterion, Cp*Ru(κ^2-*P,N*-**1**), as appealing synthetic targets (Cp* = η^5-C$_5$Me$_5$). Although well-defined, 16-electron Cp*RuL$_2^+$ complexes (L$_2$ = P$_2$- or N$_2$-donor groups) have been reported, including species that are capable of mediating substrate transformations involving C−H bond activation,[9−11] mixed P,N-ligated cations have received little attention and remain to be isolated. Furthermore, although zwitterionic complexes featuring formally cationic Ru(II) centers have been prepared,[12] none feature κ^2-*P,N* ligation, and the reactivity properties of ruthenium zwitterions have not been systematically explored. Herein we report that in contrast to the stability exhibited by the 18-electron cations Cp*Ru(CH$_3$CN)(κ^2-*P,N*-**1a**,**b**)$^+$ and the zwitterion Cp*Ru(CH$_3$CN)(κ^2-*P,N*-**1**), the related coordinatively unsaturated species Cp*Ru(κ^2-*P,N*-**1a**,**b**)$^+$ and Cp*Ru(κ^2-*P,N*-**1**) are highly reactive; Cp*Ru(κ^2-*P,N*-**1a**)$^+$ isomerizes to an η^6-species, Cp*Ru(κ^2-*P,N*-**1b**)$^+$ exhibits reversible C−H activation, and the zwitterion Cp*Ru(κ^2-*P,N*-**1**) rapidly rearranges to a Cp*Ru(H)(κ^2-*P,C*) hydridocarbene complex via ligand-assisted double geminal C−H bond activation. Data obtained in the course of NMR spectroscopic and chemical reactivity studies involving this hydridocarbene provide evidence for what appears to be the first documented interconversion of Ru(H)=CH and Ru−CH$_2$ groups by way of reversible α-hydride elimination. A portion of this work has been communicated previously.[13]

Results and Discussion

Synthesis and Characterization of Cp*Ru(Cl)(κ^2-*P,N*) and Cp*Ru(CH$_3$CN)(κ^2-*P,N*)$^+$ Complexes. Treatment of **1a** with 0.25 equiv of (Cp*RuCl)$_4$ resulted in the clean formation of Cp*Ru(Cl)(κ^2-*P,N*-**1a**) (**2a**),

(4) For selected examples, see: (a) Halcrow, M. A.; Urbanos, F.; Chaudret, B. *Organometallics* **1993**, *12*, 955. (b) Arndtsen, B. A.; Bergman, R. G. *Science* **1995**, *270*, 1970. (c) Wang, C.; Ziller, J. W.; Flood, T. C. *J. Am. Chem. Soc.* **1995**, *117*, 1647. (d) Torres, F.; Sola, E.; Martín, M.; López, J. A.; Lahoz, F. J.; Oro, L. A. *J. Am. Chem. Soc.* **1999**, *121*, 10632. (e) Tellers, D. M.; Bergman, R. G. *Organometallics* **2001**, *20*, 4819. (f) Johansson, L.; Ryan, O. B.; Rømming, C.; Tilset, M. *J. Am. Chem. Soc.* **2001**, *123*, 6579. (g) Taw, F. L.; White, P. S.; Bergman, R. G.; Brookhart, M. *J. Am. Chem. Soc.* **2002**, *124*, 4192. (h) Vedernikov, A. N.; Caulton, K. G. *Angew. Chem., Int. Ed.* **2002**, *41*, 4102. (i) Konze, W. V.; Scott, B. L.; Kubas, G. J. *J. Am. Chem. Soc.* **2002**, *124*, 12550. (j) Murakami, M.; Hori, S. *J. Am. Chem. Soc.* **2003**, *125*, 4720. (k) Dorta, R.; Goikhman, R.; Milstein, D. *Organometallics* **2003**, *22*, 2806. (l) Ackerman, L. J.; Sadighi, J. P.; Kurtz, D. M.; Labinger, J. A.; Bercaw, J. E. *Organometallics* **2003**, *22*, 3884. (m) Corkey, B. K.; Taw, F. L.; Bergman, R. G.; Brookhart, M. *Polyhedron* **2004**, *23*, 2943. (n) Ong, C. M.; Burchell, T. J.; Puddephatt, R. J. *Organometallics* **2004**, *23*, 1493. (o) Heyduk, A. F.; Driver, T. G.; Labinger, J. A.; Bercaw, J. E. *J. Am. Chem. Soc.* **2004**, *126*, 15034.

(5) (a) Helmchen, G.; Pfaltz, A. *Acc. Chem. Res.* **2000**, *33*, 336. (b) Gavrilov, K. N.; Polosukhin, A. I. *Russ. Chem. Rev.* **2000**, *69*, 661. (c) Chelucci, G.; Orrù, G.; Pinna, G. A. *Tetrahedron* **2003**, *59*, 9471.

(6) (a) Stradiotto, M.; Cipot, J.; McDonald, R. *J. Am. Chem. Soc.* **2003**, *125*, 5618. (b) Cipot, J.; Wechsler, D.; Stradiotto, M.; McDonald, R.; Ferguson M. J. *Organometallics* **2003**, *22*, 5185. (c) Wechsler, D.; McDonald, R.; Ferguson, M. J.; Stradiotto, M. *Chem. Commun*. **2004**, 2446. (d) Wile, B. M.; McDonald, R.; Ferguson, M. J.; Stradiotto, M. *Organometallics* **2005**, *24*, 1959.

(7) The reactivity of bidentate zwitterionic platinum-group metal complexes featuring either κ^2-[Ph$_2$B(CH$_2$PR$_2$)$_2$]$^-$ or κ^2-[Ph$_2$B(CH$_2$NR$_2$)$_2$]$^-$ ancillary ligands has been examined by Peters and co-workers: (a) Betley, T. A.; Peters, J. C. *Angew. Chem., Int. Ed.* **2003**, *42*, 2385. (b) Thomas, J. C.; Peters, J. C. *J. Am. Chem. Soc.* **2003**, *125*, 8870, and references therein. (c) Lu, C. C.; Peters, J. C. *J. Am. Chem. Soc.* **2004**, *126*, 15818, and references therein.

(8) (a) For a recent example of synthetically useful double C−H bond activation, see: Grotjahn, D. B.; Hoerter, J. M.; Hubbard, J. L. *J. Am. Chem. Soc.* **2004**, *126*, 8866, and references therein. (b) The conceptually related Ru-catalyzed hydrosilylation of alkenes involving double Si−H bond activation has been reported: Glaser, P. B.; Tilley, T. D. *J. Am. Chem. Soc.* **2003**, *125*, 13640.

(9) Davies, S. G.; McNally, J. P.; Smallridge, A. J. *Adv. Inorg. Chem.* **1990**, *30*, 1.

(10) (a) Nagashima, H.; Kondo, H.; Hayashida, T.; Yamaguchi, Y.; Gondo, M.; Masuda, S.; Miyazaki, K.; Matsubara, K.; Kirchner, K. *Coord. Chem. Rev.* **2003**, *245*, 177. (b) Jiménez-Tenorio, M.; Puerta, M. C.; Valerga, P. *Eur. J. Inorg. Chem.* **2004**, *17*, and references therein.

(11) Reversible activation of the C−H bonds in methane by a Cp*OsP$_2^+$ complex has been observed: Gross, C. L.; Girolami, G. S. *J. Am. Chem. Soc.* **1998**, *120*, 6605.

(12) For selected examples, see: (a) He, X. D.; Chaudret, B.; Dahan, F.; Huang, Y.-S. *Organometallics* **1991**, *10*, 970. (b) Winter, R. F.; Hornung, F. M. *Inorg. Chem.* **1997**, *36*, 6197. (c) Dioumaev, V. K.; Plössl, K.; Carroll, P. J.; Berry, D. H. *Organometallics* **2000**, *19*, 3374. (d) Mosquera, M. E. G.; Ruiz, J.; Riera, V.; Garcia-Granda, S.; Salvadó, M. A. *Organometallics* **2000**, *19*, 5533. (e) Betley, T. A.; Peters, J. C. *Inorg. Chem.* **2003**, *42*, 5074. (f) While the in situ formation of the purportedly zwitterionic complex Na[Cp*Ru(η^6-C$_9$H$_7$)SO$_3$CF$_3$] has been claimed, complete characterization data are lacking and classical resonance structure arguments obviate the need to invoke formal charge separation between the Cp*Ru and indenyl fragments in this proposed complex: Wheeler, D. E.; Bitterwolf, T. E. *Inorg. Chim. Acta* **1993**, *205*, 123.

(13) Rankin, M. A.; McDonald, R.; Ferguson, M. J.; Stradiotto, M. *Angew. Chem., Int. Ed.* **2005**, *44*, 3603.

Scheme 1. Synthesis and Isomerization of Neutral and Cationic Cp*Ru(X)(κ²-*P,N*)$^{n+}$ Complexes (X = Cl, *n* = 0; X = CH_3CN, *n* = 1)[a]

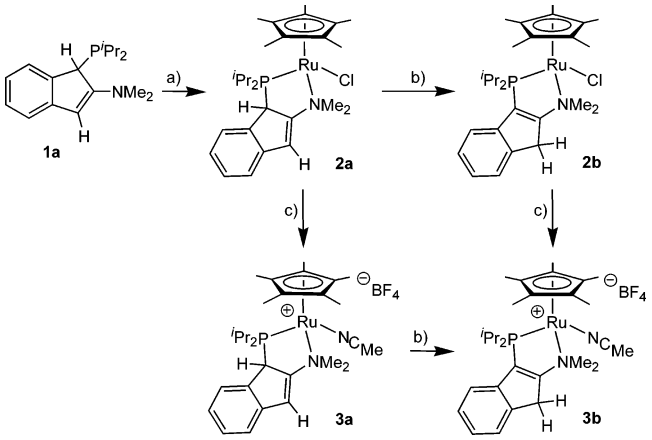

[a] Reagents: (a) 0.25 $(Cp^*RuCl)_4$; (b) NEt_3; and (c) $AgBF_4$/CH_3CN.

which in turn was isolated in 92% yield (Scheme 1). We have observed previously that solutions of **1a** slowly rearrange to a **1a**,**b** mixture on standing and that this isomerization process is accelerated to various degrees upon κ²-*P,N* coordination to a transition metal fragment and/or upon treatment with amines.[6] Benzene solutions of **2a** similarly evolved into a mixture of **2a**,**b** over 24 h, though complete conversion to **2b** required upward of four weeks. However, in the presence of triethylamine the transformation of **2a** to **2b** occurred quantitatively within 48 h, allowing for the isolation of the thermodynamically favored isomer **2b** in 85% isolated yield.[14] Data obtained from solution NMR spectroscopic and single-crystal X-ray diffraction experiments confirm the three-legged "piano-stool" structural formulations provided for both **2a** and **2b**. The crystal structures of these complexes are provided in Figure 1, and tabulated crystal data for all of the crystallographically characterized complexes reported herein are collected in Table 1. The observation of a single ^{31}P NMR resonance for **2a**, along with only one set of ^{1}H and ^{13}C resonances for each of the Cp* and κ²-*P,N*-**1a** ligands, suggests that this complex is formed in a diastereoselective fashion. In addition, both of the crystallographically independent molecules of **2a** exhibit the same relative stereochemistry at C1 and Ru, featuring *anti*-disposed C1−H and Ru−Cl units. The Ru−P and Ru−N distances both within and between **2a** and **2b** are equivalent, as are the Ru−Cl distances. The overall geometric features in **2a** and **2b** are comparable to those observed in the related complex Cp*Ru(Cl)(κ²-*P*$Ph_2CH_2CH_2N$*M*e_2).[15] In a preliminary effort to assess the stability of both **2a** and **2b** to chloride abstraction, each of these complexes was treated with $AgBF_4$ in acetonitrile. In both cases, quantitative conversion to the corresponding 18-electron, base-stabilized cation [Cp*Ru(CH_3CN)(κ²-*P,N*-**1a**,**b**)]$^+BF_4^-$ (**3a** or **3b**) was observed. These complexes were isolated in 89% and 91% yield, respectively, and were characterized; the crystallographically determined structures of **3a** and **3b** are presented in Figure 2. The

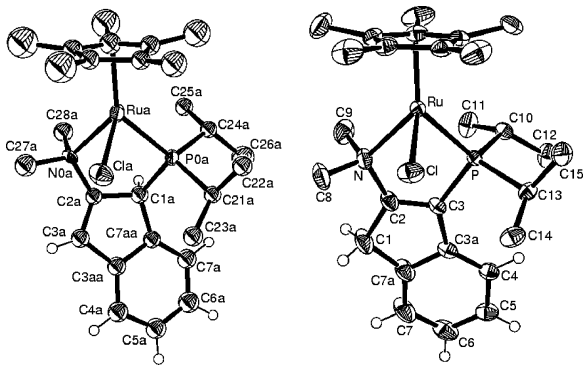

Figure 1. ORTEP diagrams for **2a** (left) and **2b** (right) shown with 50% displacement ellipsoids and with the atomic numbering scheme depicted; only one of the two independent molecules of **2a** is shown, and selected hydrogen atoms have been omitted for clarity. Selected bond lengths (Å) for **2a**: Rua−P0a 2.340(2); Rua−N0a 2.34(1); Rua−Cla 2.480(5); P0a−C1a 1.86(3); N0a−C2a 1.43(1); C1a−C2a 1.48(2); C2a−C3a 1.35(1). Selected bond lengths (Å) for **2b**: Ru−P 2.3092(5); Ru−N 2.304(2); Ru−Cl 2.4660(5); P−C3 1.813(2); N−C2 1.460(3); C1−C2 1.513(3); C2−C3 1.339(3).

stereochemical features of the ancillary P,N ligand in **3a** mirror those observed in **2a**, and there are no noteworthy differences between the related interatomic distances found within either of **3a** or **3b** and those of **2a** and **2b**. Nonlinear *Ru−N−C*CH_3 linkages such as those found in both **3a** and **3b** (168.8(2)° and 165.3(2)°, respectively) have been observed in another Cp*Ru(CH_3CN)(κ²-*P,N*)$^+$ complex.[16] As was noted for the neutral precursory chloride complexes, the cation **3a** rearranged to a **3a**,**b** mixture upon standing in acetonitrile for 12 h, with complete conversion to **3b** occurring over a two week period. However, upon exposure to triethylamine, **3a** was quantitatively transformed into **3b** within 4 h.

Pursuit of the Coordinatively Unsaturated Cation 4a. Encouraged by these preliminary synthetic experiments, we turned our attention to the preparation of the 16-electron, coordinatively unsaturated cationic complexes [Cp*Ru(κ²-*P,N*-**1a**,**b**)]$^+B(C_6F_5)_4^-$ (**4a**,**b**). Initial attempts to prepare the tetrafluoroborate analogue of **4a** via treatment of **2a** with $AgBF_4$ in either Et_2O or THF were unsuccessful, generating a complex mixture of phosphorus-containing products. Alternatively, complex **2a** was treated with $Li(Et_2O)_{2.5}B(C_6F_5)_4$ (Scheme 2). After 3 h, ^{31}P NMR analysis of the reaction mixture revealed the consumption of **2a** (δ $^{31}P = 50.0$) along with the clean formation of a single phosphorus-containing product (δ $^{31}P = 33.8$), which was isolated in 74% yield as a pale yellow solid. Given that all of the structurally authenticated $Cp^*RuN_2^+$ or $Cp^*RuP_2^+$ species are blue-purple in color,[10] we were immediately skeptical of the identity of this solid as **4a**. The observation of upfield-shifted ^{1}H and ^{13}C NMR signals confirmed this suspicion and aided in the identification of this product as the corresponding linkage isomer [Cp*Ru(η⁶-**1a**)]$^+B(C_6F_5)_4^-$ (*endo*-**4c**). Our assignment of this complex as the *endo*-isomer, in which the Cp^*Ru^+ and $^{i}Pr_2P$ groups reside on the same face of the indene fragment, is based on the observation of NOE interactions between the Cp*

(14) For rearrangements of σ-indenyl complexes, see: Stradiotto, M.; McGlinchey, M. J. *Coord. Chem. Rev.* **2001**, *219*−*221*, 311.

(15) Mauthner, K.; Slugovc, C.; Mereiter, K.; Schmid, R.; Kirchner, K. *Organometallics* **1997**, *16*, 1956.

(16) Wong, W.-K.; Chen, Y.; Wong, W.-T. *Polyhedron* **1997**, *16*, 433.

Table 1. Crystallographic Data

	2a	**2b**	**3a**	**3b**·1.5C_5H_{12}
empirical formula	$C_{27}H_{41}ClNPRu$	$C_{27}H_{41}ClNPRu$	$C_{29}H_{44}BF_4N_2PRu$	$C_{36.5}H_{62}BF_4N_2PRu$
fw	547.10	547.10	639.51	747.73
cryst dimens (mm)	0.58 × 0.43 × 0.07	0.48 × 0.15 × 0.11	0.54 × 0.32 × 0.14	0.45 × 0.29 × 0.06
cryst syst	triclinic	orthorhombic	monoclinic	monoclinic
space group	$P\bar{1}$	*Pbcn*	$P2_1/n$	$C2/c$
a (Å)	8.609(1)	30.1098(15)	11.9627(6)	22.564(2)
b (Å)	10.894(2)	8.6819(4)	14.7936(7)	17.240(2)
c (Å)	16.436(3)	19.814(1)	16.9124(8)	20.066(2)
α (deg)	113.420(3)	90	90	90
β (deg)	90.558(3)	90	91.7570(8)	109.048(1)
γ (deg)	110.862(3)	90	90	90
V (Å^3)	1301.0(4)	5179.6(4)	2991.6(3)	7378(1)
Z	2	8	4	8
ρ_{calcd} (g cm^{-3})	1.397	1.403	1.420	1.346
μ (mm^{-1})	0.782	0.785	0.623	0.516
2θ limit (deg)	52.88	52.72	52.74	52.82
	$-10 \le h \le 10$	$-37 \le h \le 37$	$-14 \le h \le 14$	$-28 \le h \le 28$
	$-13 \le k \le 13$	$-8 \le k \le 10$	$-18 \le k \le 18$	$-21 \le k \le 21$
	$-20 \le l \le 20$	$-24 \le l \le 24$	$-20 \le l \le 21$	$-25 \le l \le 25$
total no. of data collected	11 641	33 331	22 323	28 080
no. of indep reflns	11 641	5288	6112	7554
R_{int}	0	0.0346	0.0213	0.0363
no. of obsd reflns	9309	4576	5553	6141
absorp corr	multiscan (TWINABS)	multiscan (SADABS)	multiscan (SADABS)	multiscan (SADABS)
range of transmn	0.9473−0.6599	0.9186−0.7044	0.9178−0.7295	0.9697−0.8010
no. of data/restraints/params	11 641/1/294	5288/0/285	6112/0/349	7554/0/349
R_1 [$F_o^2 \ge 2\sigma(F_o^2)$]	0.0457	0.0248	0.0240	0.0370
wR_2 [$F_o^2 \ge -3\sigma(F_o^2)$]	0.1164	0.0644	0.0644	0.1102
goodness-of-fit	1.054	1.051	1.034	1.079
largest peak, hole (e Å^{-3})	0.566, −0.512	0.465, −0.214	0.573, −0.301	1.066, −0.467

	4d	**4e**	(**5a**·CH_3CN)·0.5CH_3CN	**5c**	**6**·0.5C_5H_{12}
empirical formula	$C_{51}H_{41}BF_{20}NPRu$	$C_{51}H_{41}BF_{20}NPRu$	$C_{30}H_{44.5}N_{2.5}P_1Ru_1$	$C_{27}H_{40}NPRu$	$C_{41.5}H_{57}NP_2Ru$
fw	1190.70	1190.70	572.22	510.64	732.89
cryst dimens (mm)	0.44 × 0.36 × 0.19	0.45 × 0.40 × 0.33	0.25 × 0.25 × 0.25	0.27 × 0.16 × 0.11	0.39 × 0.34 × 0.29
cryst syst	triclinic	triclinic	orthorhombic	monoclinic	triclinic
space group	$P\bar{1}$	$P\bar{1}$	*Pbca*	$P2_1/c$	$P\bar{1}$
a (Å)	12.0071(8)	10.1928(7)	13.0029(6)	14.0492(5)	11.922(1)
b (Å)	13.0736(9)	15.617(1)	24.801(1)	16.1616(6)	12.228(1)
c (Å)	16.279(1)	16.321(1)	35.844(2)	11.0248(4)	13.727(1)
α (deg)	99.1898(9)	79.3438(9)	90	90	88.894(1)
β (deg)	94.1443(9)	72.1948(9)	90	95.5325(7)	68.682(1)
γ (deg)	104.2073(9)	88.2354(9)	90	90	89.686(1)
V (Å^3)	2428.8(3)	2430.0(3)	11559.1(9)	2491.6(2)	1863.9(3)
Z	2	2	16	4	2
ρ_{calcd} (g cm^{-3})	1.628	1.627	1.315	1.361	1.306
μ (mm^{-1})	0.471	0.471	0.619	0.707	0.536
2θ limit (deg)	52.86	52.84	52.78	52.72	52.78
	$-15 \le h \le 15$	$-12 \le h \le 12$	$-16 \le h \le 16$	$-17 \le h \le 17$	$-14 \le h \le 14$
	$-16 \le k \le 16$	$-19 \le k \le 19$	$-31 \le k \le 30$	$-20 \le k \le 20$	$-15 \le k \le 15$
	$-20 \le l \le 20$	$-20 \le l \le 20$	$-44 \le l \le 44$	$-13 \le l \le 13$	$-17 \le l \le 17$
total no. of data collected	19 257	18 964	78 561	18 634	14 477
no. of indep reflns	9922	9913	11 814	5088	7581
R_{int}	0.0198	0.0152	0.0417	0.0418	0.0181
no. of obsd reflns	8818	9213	9910	4196	6905
absorp corr	Gaussian integration (face-indexed)	Gaussian integration (face-indexed)	multiscan (SADABS)	multiscan (SADABS)	Gaussian integration (face-indexed)
range of transmn	0.9159−0.8196	0.8602−0.8161	0.8616−0.8586	0.9263−0.8320	0.8601−0.8183
no. of data/restraints/params	9922/0/683	9913/0/686	11814/0/635	5088/0/288	7581/7/410
R_1 [$F_o^2 \ge 2\sigma(F_o^2)$]	0.0319	0.0256	0.0295	0.0291	0.0287
wR_2 [$F_o^2 \ge -3\sigma(F_o^2)$]	0.0909	0.0691	0.0742	0.0742	0.0801
goodness-of-fit	1.083	1.034	1.074	1.049	1.062
largest peak, hole (e Å^{-3})	0.726, −0.337	0.500, −0.315	0.356, −0.434	0.463, −0.238	0.877, −0.674

and the ^{i}Pr units in **4c**. This structural configuration is consistent with an intramolecular rearrangement mechanism in which the Ru−N and Ru−P linkages in **4a** are sequentially broken as the Cp*Ru$^+$ fragment migrates to the C_6 portion of the indene backbone. Although we cannot currently rule out alternative Cp*Ru$^+$ transfer mechanisms, consideration of steric factors alone would suggest that intermolecular pathways should preferentially lead to *exo*-**4c**; a detailed examination of this rearrangement process is currently underway.

In keeping with the allylic to vinylic isomerization processes observed for **2a** and **3a** (vide supra), in solution *endo*-**4c** slowly gives rise to [Cp*Ru(η^6-**1b**)]$^+$B(C_6F_5)$_4^-$ (**4d**), and in the presence of triethylamine this

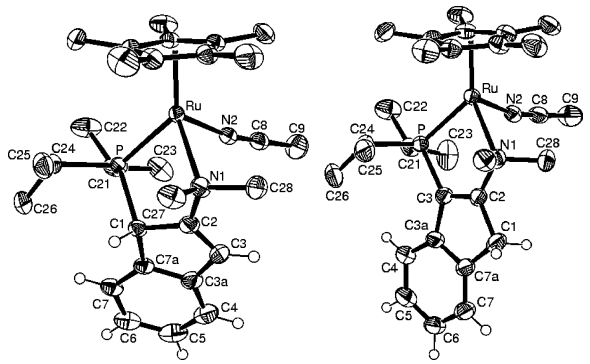

Figure 2. ORTEP diagrams for **3a** (left) and **3b**·1.5C_5H_{12} (right) shown with 50% displacement ellipsoids and with the atomic numbering scheme depicted; the tetrafluoroborate counterions, the solvates in **3b**·1.5C_5H_{12}, and selected hydrogen atoms have been omitted for clarity. Selected bond lengths (Å) and angles (deg) for **3a**: Ru−P 2.3399(4); Ru−N1 2.298(2); Ru−N2 2.052(2); P−C1 1.883(2); N−C2 1.440(2); C1−C2 1.510(2); C2−C3 1.337(3); Ru−N2−C8 168.8(2); N2−C8−C9 178.8(2). Selected bond lengths (Å) and angles (deg) for **3b**: Ru−P 2.3347(7); Ru−N1 2.283(2); Ru−N2 2.055(2); P−C3 1.822(3); N−C2 1.451(3); C1−C2 1.514(3); C2−C3 1.335(4); Ru−N2−C8 165.3(2); N2−C8−C9 178.6(4).

Scheme 2. Pursuit of the 16-Electron Cp*Ru(κ²-*P,N*)⁺ Complexes 4a and 4b[a]

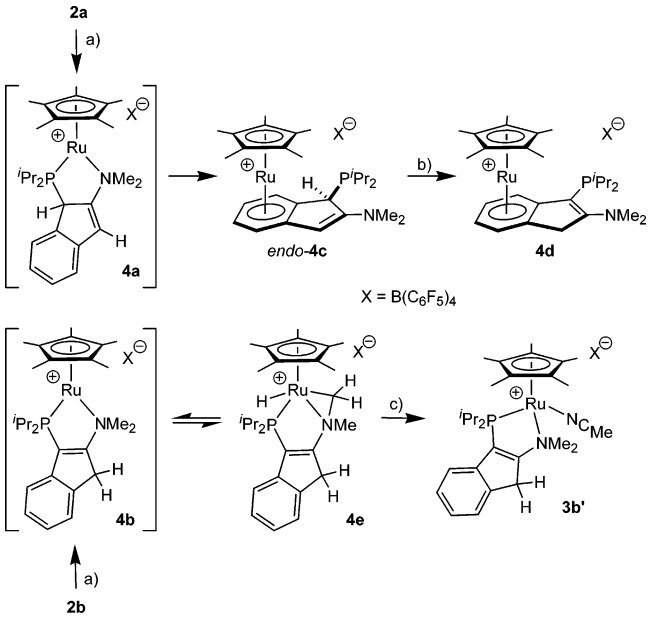

[a] Reagents: (a) $Li(Et_2O)_{2.5}B(C_6F_5)_4$; (b) NEt_3; and (c) CH_3CN.

rearrangement is quantitative after 2 h. The cation **4d** was isolated as an analytically pure pale yellow powder in 85% yield and characterized by use of NMR spectroscopic and X-ray diffraction techniques. The crystallographically determined structure of **4d** is presented in Figure 3. As has been observed in related π-complexes of polycyclic hydrocarbons,[17] the Cp^*Ru^+ fragment in **4d** is coordinated in an unsymmetrical manner to the six-membered ring of the P,N-substituted indene, with

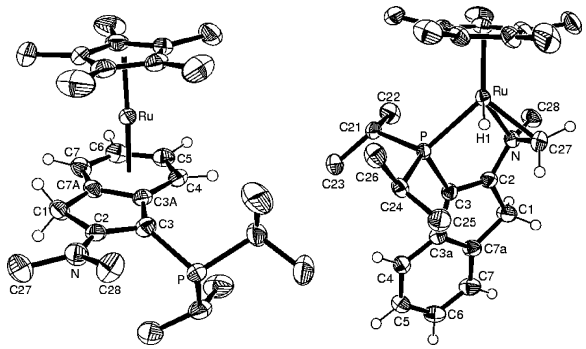

Figure 3. ORTEP diagrams for **4d** (left) and **4e** (right) shown with 50% displacement ellipsoids and with the atomic numbering scheme depicted; the tetrakis(pentafluorophenyl)borate counterions and selected hydrogen atoms have been omitted for clarity. Selected bond lengths (Å) and angles (deg) for **4d**: Ru−C3A 2.342(2); Ru−C4 2.244(2); Ru−C5 2.201(2); Ru−C6 2.197(2); Ru−C7 2.199(2); Ru−C7A 2.237(2); Ru···P 5.08; P−C3 1.833(2); C1−C2 1.508(3); C2−C3 1.393(3); N−C2 1.350(3); N−C27 1.453(3); N−C28 1.454(3); C2−N−C27 120.8(2); C2−N−C28 123.2(2); C27−N−C28 115.9(2); P−C3−C2 121.9(2); P−C3−C3A 126.6(2); C2−C3−C3A 106.8(2); N−C2−C3−P 30.4(2). Selected bond lengths (Å) and angles (deg) for **4e**: Ru−P 2.3094(4); Ru−N 2.136(1); Ru−C27 2.071(2); P−C3 1.809(2); N−C2 1.441(2); N−C27 1.433(2); N−C28 1.484(2); C1−C2 1.503(2); C2−C3 1.336(2); P−Ru−N 82.26(4); Ru−P−C3 101.90(5); Ru−N−C27 67.67(9); Ru−N−C2 116.6(1); Ru−C27−N 72.55(9).

the Ru−C3a distance (2.342(2) Å) being significantly longer than the other Ru−C_{indene} distances (∼2.22 Å). Support for the proposal that unfavorable steric interactions between the bulky Cp* and $^iPr_2P$ fragments (shortest contact ∼3.8 Å) may contribute to this distortion away from ideal η^6-coordination comes from the fact that the Cp* group is canted away from C3A, with the planes defined by the Cp* and the indene-C_6 rings deviating from a parallel arrangement by 5.3(1)°. Additionally, the $^iPr_2P$ unit in **4d** is tilted out of the plane defined by the indene-C_5 ring and away from the Cp* unit, resulting in a modest distortion toward pyramidal geometry at the formally sp^2-hybridized C3 center ($\Sigma_{angles\ at\ C3} \approx 355°$). The short N−C2 distance (1.350(3) Å) and the observed planarity at nitrogen ($\Sigma_{angles\ at\ N} \approx 360°$) suggest that the uncoordinated NMe_2 group in **4d** is in partial conjugation with the indene framework, as has been observed in some other crystallographically characterized 2-dialkylaminoindenes.[6,18] The presence of an uncoordinated NMe_2 fragment in **4d** is also consistent with the observation of equivalent NMe ^1H and ^{13}C resonances for this complex, which results from a rotation/inversion process that is rapid on the NMR time scale at 300 K.

Preparation of a Masked Form of the Coordinatively Unsaturated Cation 4b. With the goal of preparing [Cp*Ru(κ²-*P,N*-**1b**)]$^+B(C_6F_5)_4^-$ (**4b**), complex **2b** was treated with $Li(Et_2O)_{2.5}B(C_6F_5)_4$; ^{31}P NMR analysis of the reaction mixture after 1.5 h revealed the clean conversion of **2b** (δ ^{31}P = 54.0) to a single phosphorus-containing product (δ ^{31}P = 82.3), which

(17) (a) O'Connor, J. M.; Friese, S. J.; Tichenor, M. *J. Am. Chem. Soc.* **2002**, *124*, 3506. (b) Vecchi, P. A.; Alvarez, C. M.; Ellern, A.; Angelici, R. J.; Sygula, A.; Sygula, R.; Rabideau, P. W. *Angew. Chem., Int. Ed.* **2004**, *43*, 4497. (c) Takemoto, S.; Oshio, S.; Shiromoto, T.; Matsuzaka, H. *Organometallics* **2005**, *24*, 801.

(18) (a) Plenio, H.; Burth, D. *Organometallics* **1996**, *15*, 1151. (b) Plenio, H.; Burth, D. *Z. Anorg. Allg. Chem.* **1996**, *622*, 225. (c) Greidanus, G.; McDonald, R.; Stryker, J. M. *Organometallics* **2001**, *20*, 2492. (d) Cipot, J.; Wechsler, D.; McDonald, R.; Ferguson, M. J.; Stradiotto, M. *Organometallics* **2005**, *24*, 1737.

was isolated in 83% yield. Once again, the pale yellow coloration of this product suggested an alternative structural configuration to that of **4b**. Single-crystal X-ray diffraction analysis served to confirm the identity of this complex as **4e**, an 18-electron cyclometalated variant of **4b**, as depicted in Figure 3. The interatomic distances found within the metallacyclic ring in **4e** can be compared with other crystallographically characterized azaruthenacyclopropanes.[15,19] The apparent transformation of **4b** into **4e** is consistent with our previous observation that upon exposure to dimethyl sulfide the platinum center in (κ^2-*P*,*N*-**1a**)$PtMe_2$ irreversibly inserts into one of the NMe C−H bonds of **1a**, followed by loss of methane to yield an isolable cyclometalation product.[6d] Kirchner and co-workers have invoked a similar intramolecular C−H activation process involving the unobserved cationic species Cp*Ru(κ^2-*P*$Ph_2CH_2CH_2$*N*Me_2)$^+$, in which a transiently formed hydridoruthenium intermediate is proposed to react with CH_2Cl_2 to yield an isolable (κ^3-*P*,*N*,*C*)RuCl complex.[15] While no reaction between **4e** and CD_2Cl_2 was observed over 48 h, in THF-d_8 complex **4e** cleanly evolved into a new complex (δ ^{31}P = −3.9; corresponding to **4d**) over the course of five weeks. Alternative approaches to the synthesis of the tetrafluoroborate analogue of **4b** involving treatment of **2b** with $AgBF_4$ in THF were unsuccessful, generating a complex mixture of phosphorus-containing products.

Interestingly, solution ^{1}H and ^{13}C NMR data obtained for **4e** at 300 K are not in keeping with the C_1-symmetric solid-state structure depicted in Figure 3. Rather, a species possessing effective C_s-symmetry is observed, in which the NMe_2 ^{1}H NMR resonance is both broadened and shifted to an unusually low frequency (0.95 ppm, $\Delta\nu_{1/2}$ = 20.3 Hz; cf. 3.17 ppm, $\Delta\nu_{1/2}$ = 4.7 Hz and 2.77 ppm, $\Delta\nu_{1/2}$ = 3.7 Hz in **3b**). We attribute these observations to a reversible C−H oxidative addition process involving the NMe_2 fragment in **4e**, in which the metalated and free N−*C*−*H* fragments exchange rapidly on the NMR time scale at 300 K. Although on the basis of the available spectroscopic data we cannot conclusively rule out an alternative dynamic process involving agostic rather than cyclometalated species,[20] it is worthy of mention that the $^1J_{CH}$ observed for the NMe_2 group in **4e** (129.5 Hz) is only slightly reduced relative to those of **3b** (138.5 and 139.0 Hz). On cooling to 178 K, the ^{1}H NMR spectra of **4e** become increasingly complex and resonances attributable to nonmetalated NMe groups emerge, suggesting a slowing of the dynamic exchange process. However, over this temperature range no low-frequency ^{1}H NMR signals were observed that could be assigned to either Ru−H or agostic Ru-*H*-CH_2 fragments, and no new ^{31}P NMR resonances were detected. Upon exposure to CH_3CN, **4e** is quantitatively transformed into **4b**·CH_3CN (i.e., **3b′**), which provides indirect evidence for the reversibility of the cyclometalation process leading to **4e**. Given the apparent ability of **4b** to reversibly activate C−H bonds in an intramolecular fashion, we are currently exploring the viability of employing **4e** as a masked source of the 16-electron target cation, **4b**, for the development of new intermolecular C−H bond activation chemistry.

Scheme 3. Generation of the Hydridocarbene Complexes 5b and 5c

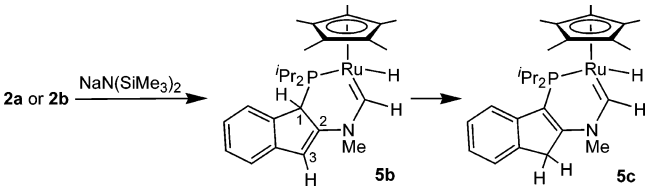

Pursuit of the Coordinatively Unsaturated Zwitterion 5a. Having successfully prepared a masked form of the coordinatively unsaturated cation **4b**, we focused our efforts on preparing the isostructural zwitterionic complex Cp*Ru(κ^2-*P*,*N*-**1**) (**5a**). Toward this end, **2a** and **2b** were separately treated with $NaN(SiMe_3)_2$ in toluene and the progress of each reaction was monitored by use of NMR methods (Scheme 3). In both cases, the initially deep red suspension of the starting materials took on a slight green coloration, which gradually evolved to red-orange over the course of 24 h; ^{31}P NMR analysis of both reaction mixtures at this stage indicated the clean conversion to a single product (δ ^{31}P = 78.2), which in turn was isolated as an orange powder in 84% yield. While elemental analysis data obtained for this isolated material were in agreement with the target zwitterion **5a**, the presence of ^{1}H NMR signals at 12.1 and −12.4 ppm, as well as a ^{13}C NMR resonance at 244.1 ppm, suggested an alternative structural formulation. The identification of this product as the hydridocarbene complex, **5c**, was confirmed on the basis of data obtained from an X-ray diffraction study. The crystallographically determined structure of **5c** is presented in Figure 4 and features a Cp*Ru(H) fragment supported by a modified form of **1b**, in which the NMe_2 unit has been trans-

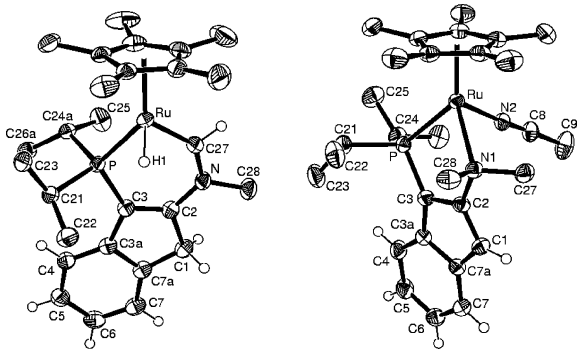

Figure 4. ORTEP diagrams for **5c** (left) and (**5a**·CH_3CN)·0.5CH_3CN (right), shown with 50% displacement ellipsoids and with the atomic numbering scheme depicted; selected hydrogen atoms and the solvate in (**5a**·CH_3CN)·0.5CH_3CN have been omitted for clarity, and only one of the two independent molecules of this complex is shown. Selected bond lengths (Å) and angles (deg) for **5c**: Ru−P 2.2374(7); Ru···N 3.05; Ru−C27 1.886(2); P−C3 1.812(2); N−C2 1.384(3); N−C27 1.374(3); N−C28 1.475(3); C1−C2 1.512(3); C2−C3 1.362(3); Ru−P−C3 112.74(9); C2−N−C27 123.5(2); C2−N−C28 117.1(2); C27−N−C28 119.4(2); N−C2−C3 129.3(2); P−C3−C2 122.7(2); Ru−C27−N 138.3(2). Selected bond lengths (Å) and angles (deg) for **5a**·CH_3CN: Ru−P 2.3645(6); Ru−N1 2.262(2); Ru−N2 2.051(2); P−C3 1.777(2); N−C2 1.467(3); C1−C2 1.383(3); C2−C3 1.413(3); Ru−N2−C8 171.5(2); N2−C8−C9 177.2(3).

(19) Liptau, P.; Carmona, D.; Oro, L. A.; Lahoz, F. J.; Kehr, G.; Erker, G. *Eur. J. Inorg. Chem.* **2004**, 4586.

(20) Brookhart, M.; Green, M. L. H.; Wong, L.-L. *Prog. Inorg. Chem.* **1988**, *36*, 1.

Scheme 4. Proposed Reaction Pathways Leading to the Hydridocarbene 5c

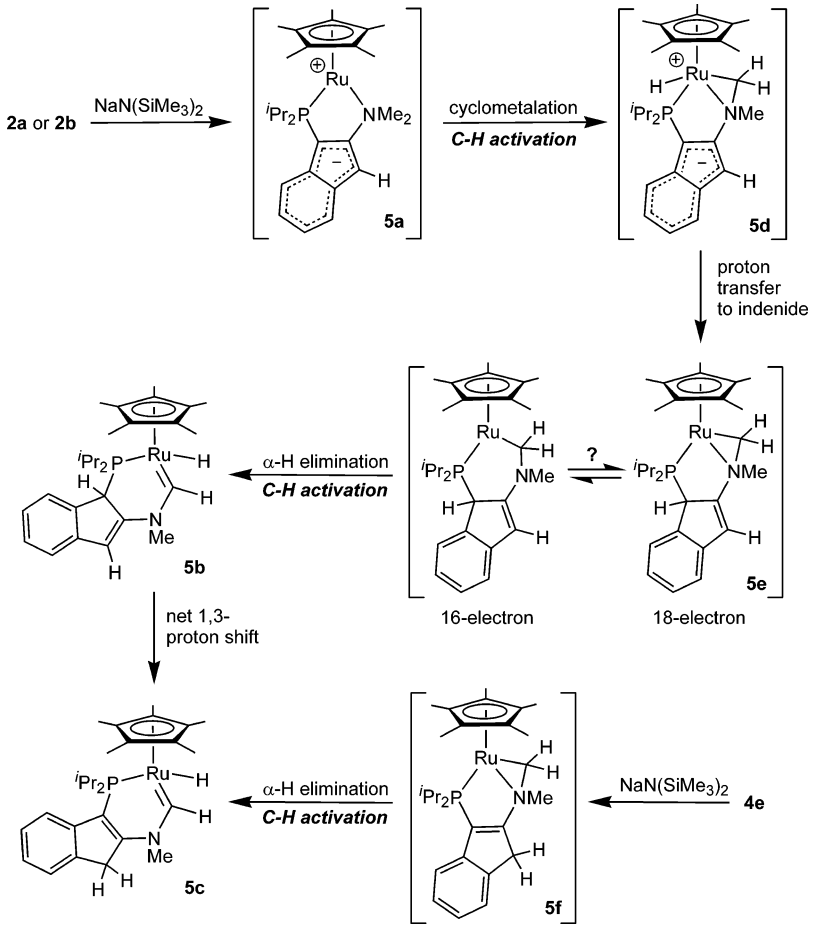

formed into a nitrogen-stabilized carbene donor group to give a κ^2-*P*,*C* complex. In **5c**, the nine carbon atoms of the indene backbone as well as C27, N, P, and Ru are essentially coplanar (max. deviation ≈ 0.3 Å), and this plane is nearly orthogonal (85.91(7)°) to the plane defined by the ring carbon atoms of the Cp* fragment. The contracted Ru−C27 (1.886(2) Å) and N−C27 (1.374(3) Å) distances in **5c** are similar to those found in some other nitrogen-stabilized carbenerutheium complexes.[21] Collectively, the aforementioned interatomic distances, the short N−C2 distance (1.384(3) Å; cf. N−C28 1.475(3) Å), and the planarity of the nitrogen center ($\sum_{\text{angles at N}} \approx 360°$) point to significant π-bonding interactions in **5c** extending from the Ru=C fragment through to the carbocyclic backbone of the indene ligand.[22]

In an attempt to learn more about the rearrangement pathway leading to **5c**, the progress of the reactions of **2a** or **2b** with $NaN(SiMe_3)_2$ in toluene were monitored by use of NMR spectroscopic techniques; both reactions yielded identical results. The ruthenium starting complex could not be detected after 20 min, with the ^{31}P NMR spectrum exhibiting new resonances at 67.8 ppm and 112.6 (**5b**) ppm (∼1:8 ratio); after 45 min only the 112.6 ppm resonance was present. Workup of the reaction at this stage allowed for the isolation of **5b** in 80% yield, and features observed in the ^1H and ^{13}C NMR spectrum allowed for the identification of this complex as the allylic isomer of **5c**. In keeping with the observed conversion of the allylic complexes **2a**, **3a**, and *endo*-**4c** to the corresponding vinylic isomers (vide supra), complex **5b** evolved cleanly into the thermodynamically favored **5c** over the course of 24 h. These spectroscopic observations are consistent with the mechanism proposed in Scheme 4, in which either **2a** or **2b** is transformed into the coordinatively unsaturated zwitterion, **5a**, upon net extrusion of HCl by $NaN(SiMe_3)_2$; cyclometalation involving an NMe C−H group subsequently produces **5d**, a zwitterionic relative of **4e**. Regioselective proton transfer (either inter- or intramolecular) from the formally cationic ruthenium center to the indenide ligand backbone gives **5e**. Detachment of the nitrogen donor in **5e** provides access to a coordinatively unsaturated alkylruthenium complex that can undergo a second C−H bond activation step (α-hydride elimination) to yield **5b**, which isomerizes to **5c**. The viability of the proposed zwitterion **5a** as a reactive intermediate en route to **5c** is supported by the fact that

(21) (a) Kuznetsov, V. F.; Yap, G. P. A.; Alper, H. *Organometallics* **2001**, *20*, 1300. (b) Ferrando-Miguel, G.; Coalter, J. N., III; Gérard, H.; Huffman, J. C.; Eisenstein, O.; Caulton, K. G. *New J. Chem.* **2002**, *26*, 687. (c) Kuznetsov, V. F.; Lough, A. J.; Gusev, D. G. *Chem. Commun.* **2002**, 2432.

(22) The reaction conditions leading to the formation of **5c** are similar to those employed in a recent series of studies in which the influence of ligand substitution pattern on the catalytic behavior of reactive species generated in situ upon treatment of Cp*Ru(Cl)(κ^2-*P*Ph_2-$CH_2CH_2NR_2$) (R = H and/or Me) with ^{t}BuOK was examined; in the case of the primary amine precursor, the coordinatively unsaturated amido complex Cp*Ru(κ^2-*P*$Ph_2CH_2CH_2$*N*H) is proposed as a key reactive intermediate: (a) Ito, M.; Osaku, A.; Kitahara, S.; Hirakawa, M.; Ikariya, T. *Tetrahedron Lett.* **2003**, *44*, 7521. (b) Ito, M.; Hirakawa, M.; Osaku, A.; Ikariya, T. *Organometallics* **2003**, *22*, 4190. (c) Ito, M.; Kitahara, S.; Ikariya, T. *J. Am. Chem. Soc.* **2005**, *127*, 6172.

the corresponding base-stabilized species **5a**·CH_3CN is an isolable complex (vide infra). Alternative mechanistic proposals involving deprotonation of an NMe group (thereby circumventing the zwitterion **5a**) can also be envisaged, and the direct conversion of **2a** to **5e** by such a pathway cannot be ruled out. By the same token, deprotonation involving an NMe group rather than the indene ring in **2b** would yield directly **5f**, the vinylic isomer of **5e**, which should evolve directly into the thermodynamically favored hydridocarbene complex **5c** *without the intermediacy of* **5b**. Such a mechanism is inconsistent with our observation that complex **5b** is the first-formed product in the reaction of the vinylic isomer **2b** with $NaN(SiMe_3)_2$, which slowly rearranges to **5c**. The rapid ligand-assisted double geminal C−H bond activation process that apparently transforms the zwitterion **5a** into the hydridocarbene **5b** at ambient temperature is noteworthy, since double geminal C−H bond activation to give a carbeneruthenium complex is still rare and invariably requires extended heating and loss of a small molecule to facilitate the reaction.[21,23,24]

For comparison, we also examined the reaction of the cation **4e** with $NaN(SiMe_3)_2$ in toluene. The ^{31}P NMR spectrum of the reaction mixture after 30 min exhibited signals corresponding only to **5c** and the as-yet-unidentified intermediate observed in the reaction of **2a** or **2b** with $NaN(SiMe_3)_2$ (67.8 ppm); after 24 h only **5c** was detected. The distinct absence of **5b** as an observable intermediate in this reaction suggests an alternative mechanistic pathway to that described above. While deprotonation of one of the benzylic protons on the indene backbone in **4e** would in principle yield **5d** and in turn **5b** on the way to **5c**, deprotonation of the acidic Ru−H fragment in **4e** would generate **5f**, which could evolve directly to **5c** by way of α-hydride elimination.

In light of the stabilization afforded to the reactive cations **4a** and **4b** upon coordination of an acetonitrile co-ligand (as in **3a** and **3b**), and with the goal of obtaining further experimental support for the intermediacy of **5a** in the formation of **5c**, efforts were made to prepare the acetonitrile-stabilized zwitterion **5a**·CH_3CN by way of net elimination of HBF_4 from **3b** in the presence of excess K_2CO_3. For the reaction conducted in THF, ^{31}P NMR analysis confirmed the consumption of **3b** after 48 h, along with the formation of the hydridocarbene **5c** and an unidentified product (53.9 ppm). In an attempt to discourage the apparent loss of the acetonitrile co-ligand, the reaction was repeated employing acetonitrile as the solvent. Although considerably slower than the reaction conducted in THF, ^{31}P NMR analysis of the reaction carried out in acetonitrile revealed the clean transformation of **3b** into a single phosphorus-containing product (44.3 ppm, **5a**·CH_3CN) after 16 days. When **2b** was used in place of **3b**, the reaction was completed after 48 h, which allowed for the convenient isolation of **5a**·CH_3CN as an analytically pure yellow-orange crystalline solid in 83% yield (eq 1). The structure of **5a**·CH_3CN was elucidated by use of NMR spectroscopic and X-ray diffraction techniques, and the crystallographically determined structure of **5a**·CH_3CN is presented in Figure 4. The structural features of the metal coordination sphere in this zwitterionic species mirror those observed in the structurally analogous cation, **3b**. However, in contrast to the bond length alternation observed in the indene portion of the ancillary ligand of **3b**, the anionic carbocyclic backbone of κ^2-*P*,*N*-**1** in **5a**·CH_3CN exhibits a more delocalized structure in keeping with a 10π-electron indenide unit, as is found in the related zwitterion (η^4-COD)Rh(κ^2-*P*,*N*-**1**).[6a] Although the *formally* zwitterionic **5a**·CH_3CN lacks a classical resonance structure that places the anionic charge onto either of the N- or P-donor fragments, the contracted P−C3 and C1−C2 distances in **5a**·CH_3CN (1.777(2) and 1.383(3) Å), when compared with those in **3b** (1.822(3) and 1.514(3) Å), indicate that a less-conventional resonance contributor featuring a P═C3 bond, which places the anionic charge on phosphorus, may also figure importantly in **5a**·CH_3CN.[25] As was noted in the reaction of **3b** with K_2CO_3 in THF, in solution (THF, benzene, or hexanes) **5a**·CH_3CN evolved cleanly into **5c** over the course of 20 h. In monitoring the progress of this transformation in benzene, only the intermediate **5b** was detected after 75 min (^{31}P NMR), in keeping with the reaction pathway outlined in Scheme 4, in which the coordinatively unsaturated zwitterion **5a** (formed in situ upon loss of acetonitrile from **5a**·CH_3CN) is transformed by way of double geminal C−H bond activation into **5b**, which in turn cleanly rearranges to **5c**. The facile dissociation of acetonitrile from **5a**·CH_3CN upon dissolution in benzene contrasts the stability observed for the isostructural cation **3b** in this solvent, which reflects the heightened electrophilicity anticipated for the formally cationic ruthenium center in **3b** relative to that in the zwitterion, **5a**·CH_3CN.

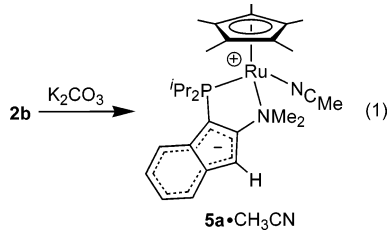

(1)

In the course of surveying the reactivity properties of **5c** with various small molecule substrates, we noted that upon exposure to $PHPh_2$ this hydridocarbene is quantitatively converted to **6**, which was subsequently isolated as an analytically pure yellow solid in 70% yield. The two phosphorus nuclei in **6** give rise to ^{31}P NMR signals at 45.1 and 54.2 ppm, and solution ^1H and ^{13}C NMR data fully support the structural formulation provided for **6** in Scheme 5. In addition, the connectivity in **6** was confirmed on the basis of data obtained from a single-crystal X-ray diffraction study; the crystallographically determined structure of **6** is presented in Figure 5. In keeping with structural features noted for

(23) (a) Coalter, J. N., III; Huffman, J. C.; Caulton, K. G. *Chem. Commun.* **2001**, 1158. (b) Ho, V. M.; Watson, L. A.; Huffman, J. C.; Caulton, K. G. *New. J. Chem.* **2003**, *27*, 1446, and references therein.

(24) A related double C−H bond activation process involving $^i Pr_2PCH_2CH_2NMe_2$ to give a nitrogen-stabilized κ^2-*P*,*C* carbeneosmium complex was observed to occur in refluxing benzene over 72 h, with net loss of H_2: Werner, H.; Weber, B.; Nürnberg, O.; Wolf, J. *Angew. Chem., Int. Ed. Engl.* **1992**, *31*, 1025.

(25) The ability of phosphorus-containing fragments to stabilize adjacent carbanions is well-established, see: Izod, K. *Coord. Chem. Rev.* **2002**, *227*, 153, and references therein.

Scheme 5. Reversible α-Hydride Elimination and Reactivity Involving the Hydridocarbene 5c

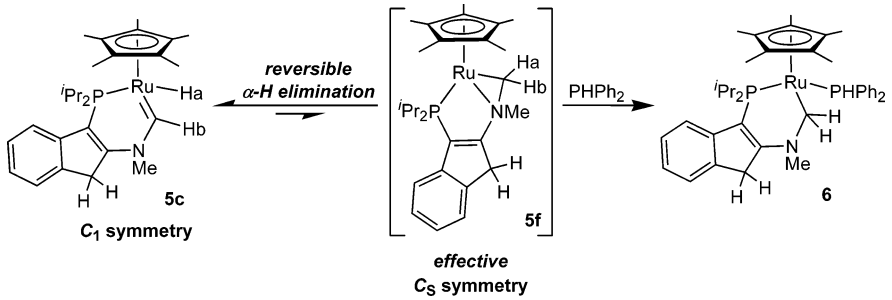

4d and **5c**, the planarity of the uncoordinated nitrogen center ($\Sigma_{\text{angles at N}} \approx 359°$) and the contracted N−C2 distance (1.338(3) Å) in **6** are indicative of π-conjugation involving the nitrogen lone pair and the adjacent indene fragment. In contrast to the nitrogen-stabilized hydridocarbene **5c**, complex **6** can be described as a base-stabilized 16-electron alkylruthenium complex, which exhibits Ru−C27 (2.124(2) Å) and N−C27 (1.469(3) Å) distances that are both lengthened significantly relative to those in **5c**.

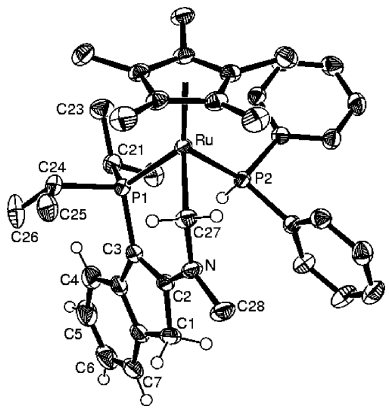

Figure 5. ORTEP diagram **6**·0.5C_5H_{12}, shown with 50% displacement ellipsoids and with the atomic numbering scheme depicted; selected hydrogen atoms and the pentane solvate have been omitted for clarity. Selected bond lengths (Å) and angles (deg) for **6**: Ru−P1 2.3031(6); Ru−P2 2.2453(5); Ru−C27 2.124(2); P1−C3 1.807(2); N−C2 1.338(3); N−C27 1.469(3); N−C28 1.472(3); C1−C2 1.516(3); C2−C3 1.397(3); P1−Ru−P2 88.43(2); P1−Ru−C27 84.74(6); P2−Ru−C27 88.02(6); C2−N−C27 123.8(2); C2−N−C28 119.5(2); C27−N−C28 115.7(2); N−C2−C3 130.5(2); P1−C3−C2 122.2(2).

A Reversible α-Hydride Elimination Process Involving Ruthenium. The transformation of **5c** into **6** upon addition of $PHPh_2$ can be viewed as involving a 1,2-hydride shift from ruthenium to the carbene carbon in **5c**, a rearrangement that is reminiscent of a 1,2-$SiMe_3$ shift process reported by Hayashida and Nagashima,[26] in which a Ru($SiMe_3$)=CH species is reversibly transformed into the corresponding (CO)-Ru-C(H)($SiMe_3$) complex upon exposure to CO. In this context we became interested in determining if the introduction of $PHPh_2$ was required in order to promote a ruthenium-to-carbene 1,2-hydride shift in **5c**, or if a dynamic, reversible α-hydride elimination process leading to the interconversion of Ru(H)=CH and Ru−CH_2 fragments (as in **5c** and **5f**, Scheme 5) was operational, even in the absence of an added Lewis base. In contrast to the well-established reversibility of β-hydride eliminations, documented examples of reversible α-hydride elimination are few,[27] and to the best of our knowledge no such reversible α-hydride elimination process involving ruthenium has been documented previously. Data obtained from 1D- and 2D-EXSY ^{1}H NMR experiments conducted at 300 K involving **5c** provided definitive spectroscopic evidence for the operation of a reversible α-hydride elimination process.[28] In the case of ^{1}H EXSY experiments employing mixing times of 0.3, 1.0, or 1.5 s, irradiation of either the Ru(*H*)=CH or the Ru(H)=C*H* signal in **5c** resulted in significant positively phased enhancement of the other resonance, indicating that these two sites are participating in chemical exchange. Features of the ^{1}H−^{1}H EXSY spectrum of **5c** (Figure 6) are also consistent with a reversible α-hydride elimination process; positive-intensity signals are shown in blue (the diagonal and the cross-peaks arising due to chemical exchange), while negative-intensity signals are shown in red (NOE cross-peaks). Positively phased off-diagonal cross-peaks (A, in Figure 6) connecting the two Ru(*H*)=C*H* environments are indicative of a chemical exchange process involving these sites. Moreover, the observation of exchange cross-peaks linking the P(C*H*$Me_a$$Me_b$)(C*H*$Me_c$$Me_d$) resonances (B, in Figure 6) are in keeping with the reversible formation of a C_s-symmetric intermediate such as **5f**. Although we would also expect to observe exchange cross-peaks linking the P(CH*Me*$_2$)$_2$ and indene-C*H*$_2$ environments (respectively), these resonances are not sufficiently resolved so as to allow for the conclusive identification of off-diagonal correlations. The documentation of a reversible α-hydride elimination process involving ruthenium is significant, since the interconversion of Ru=C and Ru-alkyl

(26) Hayashida, T.; Nagashima, H. *Organometallics* **2001**, *20*, 4996.

(27) For selected examples, see: (a) Cooper, N. J.; Green, M. L. H. *J. Chem. Soc., Dalton Trans.* **1979**, 1121. (b) Threlkel, R. S.; Bercaw, J. E. *J. Am. Chem. Soc.* **1981**, *103*, 2650. (c) Turner, H. W.; Schrock, R. R.; Fellmann, J. D.; Holmes, S. J. *J. Am. Chem. Soc.* **1983**, *105*, 4942. (d) van Asselt, A.; Burger, B. J.; Gibson, V. C.; Bercaw, J. E. *J. Am. Chem. Soc.* **1986**, *108*, 5347. (e) Parkin, G.; Bunel, E.; Burger, B. J.; Trimmer, M. S.; van Asselt, A.; Bercaw, J. E. *J. Mol. Catal.* **1987**, *41*, 21. (f) Luecke, H. F.; Arndtsen, B. A.; Burger, P.; Bergman, R. G. *J. Am. Chem. Soc.* **1996**, *118*, 2517. (g) Schrock, R. R.; Seidel, S. W.; Mösch-Zanetti, N. C.; Shih, K.-Y.; O'Donoghue, M. B.; Davis, W. M.; Reiff, W. M. *J. Am. Chem. Soc.* **1997**, *119*, 11876. (h) Carmona, E.; Paneque, M.; Poveda, M. L. *Dalton Trans.* **2003**, 4022. (i) Clot, E.; Chen, J.; Lee, D.-H.; Sung, S. Y.; Appelhans, L. N.; Faller, J. W.; Crabtree, R. H.; Eisenstein, O. *J. Am. Chem. Soc.* **2004**, *126*, 8795, and references therein. (j) Paneque, M.; Poveda, M. L.; Santos, L. L.; Carmona, E.; Lledós, A.; Ujaque, G.; Mereiter, K. *Angew. Chem., Int. Ed.* **2004**, *43*, 3708. (k) For a recent example in which facile reversible α-hydride elimination involving ruthenium has been invoked, see: Gusev, D. G.; Lough, A. J. *Organometallics* **2002**, *21*, 2601.

(28) For discussions regarding 1D- and 2D-exchange spectroscopy (EXSY) NMR, see: (a) Perrin, C. L.; Dwyer, T. J. *Chem. Rev.* **1990**, *90*, 935, and references therein. (b) Perrin, C. L.; Engler, R. E. *J. Am. Chem. Soc.* **1997**, *119*, 585, and references therein.

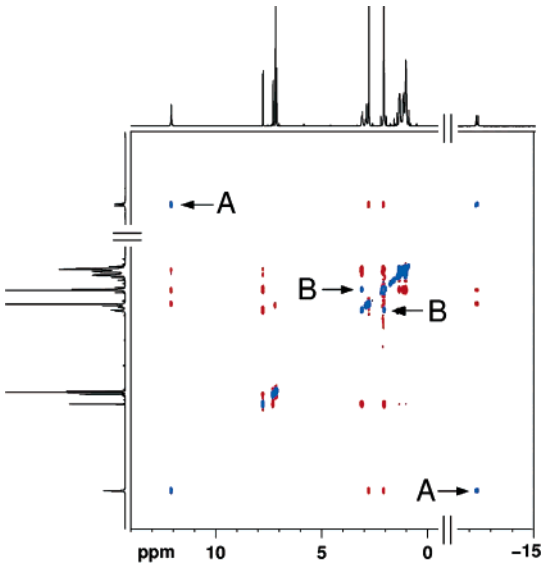

Figure 6. $^1H-^1H$ EXSY spectrum of **5c** (300 K; 0.8 s mixing time); the spectrum has been truncated for clarity. Positive-intensity signals are shown in blue (the diagonal and EXSY cross-peaks), while negative-intensity signals are shown in red (NOE cross-peaks). The off-diagonal cross-peaks identified as A and B indicate chemical exchange of the Ru(*H*)=C*H* environments, as well as the P(C*H*$Me_a$$Me_b$)(C*H*$Me_c$$Me_d$) sites, respectively.

species by this mechanism may play a role in the inadvertent transmutation of olefin metathesis and hydrogenation catalysts in situ.[29,30]

Summary and Conclusions

Whereas the coordinatively saturated, base-stabilized 18-electron complexes Cp*Ru(CH_3CN)(κ^2-*P*,*N*-**1a**,**b**)$^+$ and Cp*Ru(CH_3CN)(κ^2-*P*,*N*-**1**) are isolable species, in the absence of a stabilizing acetonitrile co-ligand more aggressive reactivity behavior is observed. The putative 16-electron cation Cp*Ru(κ^2-*P*,*N*-**1a**)$^+$ rapidly rearranges to the linkage isomer Cp*Ru(η^6-**1a**)$^+$, while the isomeric cation Cp*Ru(κ^2-*P*,*N*-**1b**)$^+$ maintains a κ^2-*P*,*N* configuration and reversibly inserts into the C−H bonds of the NMe_2 group. Moreover, the related coordinatively unsaturated zwitterion Cp*Ru(κ^2-*P*,*N*-**1**) has proven capable of double geminal C−H bond activation under rather mild conditions to ultimately give the 18-electron κ^2-*P*,*C* hydridocarbene, **5c**, a transformation that is enabled by the proton-accepting ability of the anionic indenide fragment in **1**. An NMR spectroscopic study involving **5c** revealed that the second C−H activation step leading to the formation of this hydridocarbene is reversible; notably, this observation appears to represent the first documented example of such a reversible α-hydride elimination process involving ruthenium. Given the current interest both in the development of bidentate phosphine-carbene ligands for use in homogeneous catalytic applications[31] and in the establishment of mild synthetic routes to carbenemetal complexes based on C−H bond activation,[32] we are currently exploring the generality of employing **1** as a precursor to other κ^2-*P*,*C* carbenemetal species.

The divergent C−H bond activation behavior observed for the structurally related series Cp*Ru(κ^2-*P*,*N*-**1a**)$^+$ (*no* C−H activation), Cp*Ru(κ^2-*P*,*N*-**1b**)$^+$ (*single* C−H activation), and Cp*Ru(κ^2-*P*,*N*-**1**) (*double* C−H activation) is remarkable and serves to highlight how seemingly subtle alterations to the steric and electronic properties of an ancillary ligand can translate into profoundly different reactivity characteristics exhibited by the associated coordinatively unsaturated metal complexes. In addition, while 16-electron $CpRuL_2^+$ species are commonly invoked as reactive intermediates in a variety of prominent synthetic transformations,[9,10,33] the observations described herein underscore the inherent limitations associated with developing detailed structure−activity relationships through the examination of such coordinatively unsaturated species generated in situ.

Encouraged by the demonstrated ability of Cp*Ru(κ^2-*P*,*N*-**1b**)$^+$ and Cp*Ru(κ^2-*P*,*N*-**1**) to activate C−H bonds in an intramolecular fashion, we are currently developing analogues of these coordinatively unsaturated complexes that feature more metalation-resistant κ^2-*P*,*N* ancillary ligands, with the aim of developing new metal-mediated intermolecular C−H bond activation processes. In this context we are particularly interested in exploring the possibility of exploiting **1** and related donor-functionalized indenide ligands as *reversible* proton acceptors in the establishment of synthetically useful reaction chemistry based on multiple C−H bond activation.

Experimental Section

General Considerations. All manipulations were conducted in the absence of oxygen and water under an atmosphere of dinitrogen, either by use of standard Schlenk methods or within an mBraun glovebox apparatus, utilizing glassware that was oven-dried (130 °C) and evacuated while hot prior to use. Celite (Aldrich) was oven-dried (130 °C) for 5 days and then evacuated for 24 h prior to use. The nondeuterated solvents dichloromethane, diethyl ether, toluene, benzene, and pentane were deoxygenated and dried by sparging with dinitrogen gas, followed by passage through a double-column solvent purification system provided by mBraun Inc. Dichloromethane and diethyl ether were purified over two alumina-packed columns, while toluene, benzene, and pentane were purified over one alumina-packed column and one column packed with copper-Q5 reactant. Purification of acetonitrile was achieved by refluxing over CaH_2 for 4 days under dinitrogen, followed by distillation. Purification of triethylamine was achieved by stirring over KOH for 7 days, followed by distillation; the distilled triethylamine was then refluxed over CaH_2 for 3 days under dinitrogen, followed by distillation. C_6D_6 and THF-d_8 (Aldrich) were degassed by using three

(29) (a) The unintentional interconversion of catalytically active Ru=C, Ru−R, and Ru−H complexes in situ is well documented, see: Schmidt, B. *Eur. J. Org. Chem.* **2004**, 1865. (b) As well, the rational tranformation of Ru=C olefin metathesis catalysts into hydrogenation catalysts has enabled the development of highly efficient "one-pot" tandem catalysis procedures, see: Louie, J.; Bielawski, C. W.; Grubbs, R. H. *J. Am. Chem. Soc.* **2001**, *123*, 11312.

(30) For discussions of metal-alkyl/metal-alkylidene equilibria, see: (a) Caulton, K. G. *J. Organomet. Chem.* **2001**, *617*−*618*, 56. (b) ref 27h.

(31) (a) For example: Danopoulos, A. A.; Winston, S.; Gelbrich, T.; Hursthouse, M. B.; Tooze, R. P. *Chem. Commun.* **2002**, 482. (b) For a recent report featuring ruthenium complexes supported by phosphine-functionalized *N*-heterocyclic carbene ligands, see: Gischig, S.; Togni, A. *Organometallics* **2004**, *23*, 2479.

(32) Viciano, M.; Mas-Marzá, E.; Poyatos, M.; Sanaú, M.; Crabtree, R. H.; Peris, E. *Angew. Chem., Int. Ed.* **2005**, *44*, 444, and references therein.

(33) Trost, B. M. *Acc. Chem. Res.* **2002**, *35*, 695.

repeated freeze−pump−thaw cycles and then dried over 3 Å molecular sieves for 24 h prior to use. All solvents used within the glovebox were stored over activated 3 Å molecular sieves. Compounds **1a**[6a] and $(Cp^*RuCl)_4$[34] were prepared by employing published procedures. All other commercial reagents were obtained from Aldrich and were used as received, with the exception that $AgBF_4$ was dried in vacuo for 12 h prior to use, $PHPh_2$ was obtained from Alpha Aesar, and $Li(Et_2O)_{2.5}B(C_6F_5)_4$ was obtained from Boulder Scientific. Unless otherwise stated, ^1H, ^{13}C, and ^{31}P NMR characterization data were collected at 300 K on a Bruker AV-500 spectrometer operating at 500.1, 125.8, and 202.5 MHz (respectively) with chemical shifts reported in parts per million downfield of $SiMe_4$ (for ^1H and ^{13}C) or 85% H_3PO_4 in D_2O (for ^{31}P). In some cases slightly fewer than expected independent ^1H or ^{13}C NMR resonances were observed (despite prolonged data acquisition times), and resonances associated with $B(C_6F_5)_4^-$ were not assigned. ^1H and ^{13}C NMR chemical shift assignments and $^1J_{CH}$ determinations are based on data obtained from ^{13}C-DEPT, $^1H-^1H$ COSY, $^1H-^{13}C$ HSQC, and $^1H-^{13}C$ HMBC NMR experiments. Elemental analyses were performed by Canadian Microanalytical Service Ltd., Delta, British Columbia, Canada.

Synthesis of 2a. To a glass vial containing a magnetically stirred solution of $(Cp^*RuCl)_4$ (0.25 g, 0.23 mmol) in CH_2Cl_2 (5 mL) was added solid **1a** (0.25 g, 0.92 mmol) all at once. The addition caused an immediate color change from dark brown to dark red. The vial was then sealed with a PTFE-lined cap, and the solution was magnetically stirred for 45 min. ^{31}P NMR data collected on an aliquot of this solution indicated the quantitative formation of **2a**. The CH_2Cl_2 solvent was then removed in vacuo, yielding a dark red oily solid. The solid was then triturated with pentane (1.5 mL), and the pentane was removed in vacuo to yield **2a** as an analytically pure orange-pink powder (0.46 g, 0.85 mmol, 92%). Anal. Calcd for $C_{27}H_{41}PNRuCl$: C 59.27; H 7.55; N 2.56. Found: C 59.02; H 7.48; N 2.73. ^1H NMR (C_6D_6): δ 7.24−7.05 (m, 4H, aryl-Hs), 5.89 (s, 1H, C3−H), 3.92 (d, $^2J_{PH}$ = 8.5 Hz, 1H, C1−H), 2.86 (s, 3H, NMe_a), 2.72 (s, 3H, NMe_b), 2.50 (m, 1H, P(C*H*Me_aMe_b)), 2.26 (m, 1H, P(C*H*Me_cMe_d)), 1.51 (s, 15H, C_5Me_5), 1.31−1.22 (m, 6H, P(CH*Me*$_cMe_d$)), 1.01 (d of d, $^3J_{PH}$ = 17.0 Hz, $^3J_{HH}$ = 7.0 Hz, 3H, P(CH*Me*$_aMe_b$)), 0.90 (d of d, $^3J_{PH}$ = 13.5 Hz, $^3J_{HH}$ = 7.0 Hz, 3H, P(CHMe$_a$*Me*$_b$)). $^{13}C\{^1H\}$ NMR (C_6D_6): δ 166.1 (d, $^2J_{PC}$ = 5.3 Hz, C2), 144.8 (C3a), 138.8 (d, $^2J_{PC}$ = 6.3 Hz, C7a), 126.8 (aryl-*C*H), 123.8 (aryl-*C*H), 123.7 (aryl-*C*H), 121.4 (aryl-*C*H), 114.6 (d, $^3J_{PC}$ = 5.9 Hz, C3), 79.6 (C_5Me_5), 56.0 (NMe_b), 48.0 (NMe_a), 44.9 (C1), 28.0 (d, $^1J_{PC}$ = 15.6 Hz, P(*C*HMe_aMe_b)), 24.5 (d, $^1J_{PC}$ = 15.5 Hz, P(*C*HMe_cMe_d)), 21.1 (d, $^2J_{PC}$ = 6.4 Hz, P(CH*Me*$_cMe_d$) or P(CHMe$_c$*Me*$_d$)), 20.4 (P(CHMe$_a$*Me*$_b$)), 19.0−18.8 (m, P(CH*Me*$_aMe_b$) and either P(CH*Me*$_cMe_d$) or P(CHMe$_c$*Me*$_d$)), 10.8 (s, C_5Me_5). $^{31}P\{^1H\}$ NMR (C_6D_6): δ 50.0. A crystal of **2a** suitable for single-crystal X-ray diffraction studies was grown from a pentane solution at −35 °C.

Synthesis of 2b. To a glass vial containing a magnetically stirred solution of freshly prepared **2a** (0.50 g, 0.92 mmol) in C_6H_6 (8 mL) was added NEt_3 (1.5 mL). The vial was then sealed with a PTFE-lined cap, and the solution was magnetically stirred for 48 h. ^{31}P NMR data collected on an aliquot of this solution indicated clean conversion to **2b**. The C_6H_6 solvent and other volatile materials were then removed in vacuo, yielding a dark red oily solid. The solid was then washed with cold pentane (2 × 1.5 mL, precooled to −35 °C), and the product was then dried in vacuo to yield **2b** as an analytically pure orange-pink powder (0.43 g, 0.78 mmol, 85%). Anal. Calcd for $C_{27}H_{41}PNRuCl$: C 59.27; H 7.55; N 2.56. Found: C 59.27; H 7.47; N 2.68. ^1H NMR (C_6D_6): δ 7.52 (d, $^3J_{HH}$ = 7.5 Hz, 1H, C4−H or C7−H), 7.22 (t, $^3J_{HH}$ = 7.0 Hz, 1H, C5−H or C6−H), 7.17−7.08 (m, 2H, aryl-Hs), 3.05 (m, 1H, P(C*H*Me_aMe_b)), 2.97 (br s, 3H, NMe_a), 2.80−2.63 (m, 5H, NMe_b and C(*H*$_a$)(*H*$_b$)), 2.49 (m, 1H, P(C*H*Me_cMe_d)), 1.65 (m, 3H, P(CH*Me*$_aMe_b$)), 1.61 (s, 15H, C_5Me_5), 1.45 (d of d, $^3J_{PH}$ = 18.0 Hz, $^3J_{HH}$ = 6.5 Hz, 3H, P(CHMe$_a$*Me*$_b$)), 1.25 (d of d, $^3J_{PH}$ = 11.0 Hz, $^3J_{HH}$ = 7.0 Hz, 3H, P(CH*Me*$_cMe_d$)), 1.14 (d of d, $^3J_{PH}$ = 15.5 Hz, $^3J_{HH}$ = 7.5 Hz, 3H, P(CHMe$_c$*Me*$_d$)). $^{13}C\{^1H\}$ NMR (C_6D_6): δ 176.1 (d, $^2J_{PC}$ = 19.6 Hz, C2), 143.5 (d, J_{PC} = 4.0 Hz, C3a or C7a), 142.6 (d, J_{PC} = 4.0 Hz, C7a or C3a), 135.2 (d, $^1J_{PC}$ = 16.7 Hz, C3), 126.5 (C5 or C6), 124.7 (C4 or C7 and either C6 or C5), 123.3 (C7 or C4), 79.5 (d, J = 2.3 Hz, C_5Me_5), 58.2 (br m, NMe_b), 51.4 (br m, NMe_a), 30.3 (d, $^3J_{PC}$ = 7.5 Hz, C1), 27.8 (d, $^1J_{PC}$ = 19.1 Hz, P(*C*HMe_cMe_d)), 27.0 (d, $^1J_{PC}$ = 24.7 Hz, P(*C*HMe_aMe_b)), 22.0 (P(CH*Me*$_aMe_b$)), 20.9 (d, $^2J_{PC}$ = 5.7 Hz, P(CHMe$_c$*Me*$_d$)), 20.5−20.3 (m, P(CHMe$_a$*Me*$_b$) and P(CH*Me*$_cMe_d$)), 10.9 (C_5Me_5). $^{31}P\{^1H\}$ NMR (C_6D_6): δ 54.0. A crystal of **2b** suitable for single-crystal X-ray diffraction studies was grown from a CH_2Cl_2 solution at −35 °C.

Synthesis of 3a. To a glass vial containing a magnetically stirred orange solution of **2a** (0.20 g, 0.37 mmol) in MeCN (4 mL) was added solid $AgBF_4$ (0.072 g, 0.37 mmol) all at once. The addition caused an immediate formation of a precipitate. The vial was then sealed with a PTFE-lined cap, and the solution was magnetically stirred for 30 min. ^{31}P NMR data collected on an aliquot of this crude reaction mixture indicated the quantitative formation of **3a**. The reaction mixture was then filtered through Celite, yielding a yellow solution. The solvent and other volatile materials were subsequently removed in vacuo, yielding a waxy yellow solid. The solid was then washed with pentane (5 × 1.5 mL), and the product was then dried in vacuo to yield **3a** as an analytically pure yellow powder (0.21 g, 0.33 mmol, 89%). Anal. Calcd for $C_{29}H_{44}PN_2RuCl$: C 54.46; H 6.94; N 4.38. Found: C 54.21; H 7.12; N 4.42. ^1H NMR (THF-d_8): δ 7.32−7.31 (m, 2H, C4−H and C7−H), 7.16 (t, $^3J_{HH}$ = 7.5 Hz, 1H, C5−H), 7.01 (t, $^3J_{HH}$ = 7.5 Hz, 1H, C6−H), 6.57 (s, 1H, C3−H), 4.50 (d, $^2J_{PH}$ = 10.0 Hz, 1H, C1−H), 3.17 (s, 3H, NMe_a), 2.97 (s, 3H, NMe_b), 2.66−2.56 (m, 2H, P(C*H*Me_aMe_b) and P(C*H*Me_cMe_d)), 2.47 (s, 3H, MeCN), 1.65 (s, 15H, C_5Me_5), 1.62−1.55 (m, 6H, P(CH*Me*$_aMe_b$)), 1.07 (d of d, $^3J_{PH}$ = 16.0 Hz, $^3J_{HH}$ = 7.0 Hz, 3H, P(CH*Me*$_cMe_d$)), 0.21 (d of d, $^3J_{PH}$ = 15.0 Hz, $^3J_{HH}$ = 7.0 Hz, 3H, P(CHMe$_c$*Me*$_d$)). $^{13}C\{^1H\}$ NMR (THF-d_8): δ 164.0 (d, $^2J_{PC}$ = 4.9 Hz, C2), 142.4 (C3a), 135.9 (d, $^2J_{PC}$ = 6.5 Hz, C7a), 128.1 (Me*C*N), 125.2 (C5), 122.3 (C6), 122.0 (C4 or C7), 120.3 (C7 or C4), 113.3 (d, $^3J_{PC}$ = 6.7 Hz, C3), 82.0 (C_5Me_5), 54.5 (NMe_a), 47.8 (NMe_b), 42.0 (d, $^1J_{PC}$ = 4.2 Hz, C1), 25.1 (d, $^1J_{PC}$ = 18.2 Hz, P(*C*HMe_cMe_d)), 22.0 (d, $^1J_{PC}$ = 18.6 Hz, P(*C*HMe_aMe_b)), 21.1 (d, $^2J_{PC}$ = 5.8 Hz, P(CH*Me*$_aMe_b$) or P(CHMe$_a$*Me*$_b$)), 16.9 (P(CHMe$_c$*Me*$_d$)), 16.0−15.9 (m, P(CH*Me*$_cMe_d$) and either P(CH*Me*$_aMe_b$) or P(CHMe$_a$*Me*$_b$)), 7.9 (C_5Me_5), 1.5 (*Me*CN). $^{31}P\{^1H\}$ NMR (THF-d_8): δ 44.8. A crystal of **3a** suitable for single-crystal X-ray diffraction studies was grown from a concentrated CH_2Cl_2/pentane solution at −35 °C.

Synthesis of 3b and 3b′. To a glass vial containing a magnetically stirred orange solution of **2b** (0.050 g, 0.091 mmol), in MeCN (4 mL), was added solid $AgBF_4$ (0.018 g, 0.092 mmol) all at once. The addition caused an immediate formation of a precipitate. The vial was then sealed with a PTFE-lined cap, and the solution was magnetically stirred for 30 min. ^{31}P NMR data collected on an aliquot of this crude reaction mixture indicated the quantitative formation of **3b**. The reaction mixture was then filtered through Celite, yielding a yellow solution. The solvent and other volatile materials were subsequently removed in vacuo, yielding a waxy yellow solid. The solid was then washed with pentane (5 × 1.5 mL), and the product was then dried in vacuo to yield **3b** as an analytically pure yellow powder (0.053 g, 0.083 mmol, 91%). Anal. Calcd. for $C_{29}H_{44}PN_2RuBF_4$: C 54.46; H 6.94; N 4.38. Found: C 54.59; H 6.82; N 4.11. ^1H NMR (C_6D_6): δ 7.37 (d, $^3J_{HH}$ = 7.5 Hz, 1H, C4−H or C7−H), 7.33 (d, $^3J_{HH}$ = 7.5 Hz, 1H, C7−H or C4−H), 7.22 (t, $^3J_{HH}$ = 7.0 Hz, 1H, C5−H or

(34) Fagan, P. J.; Ward, M. D.; Calabrese, J. C. *J. Am. Chem. Soc.* **1989**, *111*, 1698.

C6−H), 7.11 (m, 1H, C6−H or C5−H), 3.54 (m, 2H, C(H_a)(H_b)), 3.17 (s, 3H, NMe_a), 2.97 (m, 1H, P(C*H*$Me_a$$Me_b$)), 2.77 (s, 3H, NMe_b), 2.13−2.01 (m, 4H, P(C*H*$Me_c$$Me_d$) and MeCN), 1.40 (s, 15 H, C_5Me_5), 1.17 (d of d, $^3J_{PH}$ = 11.0 Hz, $^3J_{HH}$ = 7.0 Hz, 3H, P(CH*Me*$_c$$Me_d$)), 0.99 (d of d, $^3J_{PH}$ = 17.0 Hz, $^3J_{HH}$ = 7.0 Hz, 3H, P(CH*Me*$_a$$Me_b$)), 0.80 (d of d, $^3J_{PH}$ = 17.0 Hz, $^3J_{HH}$ = 7.5 Hz, 3H, P(CHMe_c*Me*$_d$)), 0.70 (d of d, $^3J_{PH}$ = 14.5 Hz, $^3J_{HH}$ = 7.0 Hz, 3H, P(CHMe_a*Me*$_b$)). $^{13}C\{^1H\}$ NMR (C_6D_6): δ 179.3 (d, $^2J_{PC}$ = 19.1 Hz, C2), 144.5 (d, J_{PC} = 5.4 Hz, C3a or C7a), 140.7 (C7a or C3a), 132.3 (d, $^1J_{PC}$ = 20.5 Hz, C3), 130.1 (Me*C*N), 126.4 (C5 or C6), 125.7−125.6 (m, 2 overlapping aryl-*C*Hs), 122.4 (C4 or C7), 84.1 (C_5Me_5), 59.1 (NMe_b), 54.0 (NMe_a), 31.6 (d, $^3J_{PC}$ = 7.4 Hz, C1), 26.2 (d, $^1J_{PC}$ = 20.9 Hz, P(*C*H$Me_c$$Me_d$)), 24.8 (d, $^1J_{PC}$ = 26.3 Hz, P(*C*H$Me_a$$Me_b$)), 20.5 (P(CH$Me_c$*Me*$_d$)), 19.7−19.5 (m, P(CH$Me_a$*Me*$_b$) and P(CH*Me*$_c$$Me_d$)), 18.7 (P(CH*Me*$_a$$Me_b$)), 10.2 ($C_5Me_5$), 3.8 (*Me*CN). $^{31}P\{^1H\}$ NMR (C_6D_6): δ 55.8. A crystal of **3b**·1.5C_5H_{12} suitable for single-crystal X-ray diffraction studies was grown from a toluene/pentane solution at −35 °C. Complex **3b′** was prepared in situ by dissolution of **4e** in MeCN and yielded NMR spectroscopic data identical to those reported for **3b**.

Synthesis of *endo*-4c. To a glass vial containing a magnetically stirred suspension of **2a** (0.15 g, 0.27 mmol) in Et_2O (5 mL) was added solid $Li(Et_2O)_{2.5}B(C_6F_5)_4$ (0.24 g, 0.28 mmol) all at once. The addition caused an immediate darkening of the mixture from red-orange to dark brown, and dissolution of **2a** occurred over the course of several minutes. The vial was then sealed with a PTFE-lined cap, and the solution was magnetically stirred for 3 h. Over this time period a fine white precipitate had formed, and the reaction mixture had gradually lightened in color from dark brown to yellow-brown. ^{31}P NMR data collected on an aliquot of this crude reaction mixture indicated the quantitative formation of **4c**. After filtering the mixture through Celite, the solvent and other volatile substances were removed in vacuo. The resulting oily yellow solid was washed with pentane (5 × 1.5 mL), yielding **4c** as an analytically pure pale yellow powder (0.24 g, 0.20 mmol, 74%). Anal. Calcd for $C_{51}H_{41}PNRuBF_{20}$: C 51.44; H 3.47; N 1.18. Found: C 51.16; H 3.24; N 1.09. ^1H NMR (THF-d_8): δ 6.00 (d, $^3J_{HH}$ = 5.5 Hz, 1H, C4−H or C7−H), 5.65 (d, $^3J_{HH}$ = 5.5 Hz, 1H, C7−H or C4−H), 5.37−5.33 (m, 2H, C5−H and C6−H), 5.26 (s, 1H, C3−H), 3.78 (m, 1H, C1−H), 2.83 (s, 6H, NMe_2), 2.48 (m, 1H, P(C*H*$Me_a$$Me_b$)), 2.12 (m, 1H, P(C*H*$Me_c$$Me_d$)), 1.93 (s, 15H, C_5Me_5), 1.46 (d of d, $^3J_{PH}$ = 12.0 Hz, $^3J_{HH}$ = 7.5 Hz, 3H, P(CH*Me*$_c$$Me_d$)), 1.37 (d of d, $^3J_{PH}$ = 10.0 Hz, $^3J_{HH}$ = 7.0 Hz, 3H, P(CHMe_c*Me*$_d$)), 1.13 (d of d, $^3J_{PH}$ = 13.0 Hz, $^3J_{HH}$ = 7.0 Hz, 3H, P(CH*Me*$_a$$Me_b$)), 1.07 (d of d, $^3J_{PH}$ = 16.5 Hz, $^3J_{HH}$ = 7.0 Hz, 3H, P(CHMe_a*Me*$_b$)). $^{13}C\{^1H\}$ NMR (THF-d_8): δ 164.1 (C2), 113.0 (C3a), 111.9 (d, $^2J_{PC}$ = 17.9 Hz, C7a), 92.7 (C3), 92.5 (C_5Me_5), 83.4 (C5 or C6), 80.7 (d, J_{PC} = 3.1 Hz, C4 or C7), 79.4 (C6 or C5), 74.6 (C7 or C4), 40.2 (d, $^1J_{PC}$ = 40.9 Hz, C1), 39.6 (NMe_2), 24.6 (d, $^1J_{PC}$ = 18.2 Hz, P(*C*H$Me_a$$Me_b$)), 20.6 (m, P(CH$Me_a$*Me*$_b$)), 20.1 (d, $^1J_{PC}$ = 24.7 Hz, P(*C*H$Me_c$$Me_d$)), 18.0−17.8 (P(CH*Me*$_a$$Me_b$) and P(CH*Me*$_c$$Me_d$)), 17.2 (d, $^2J_{PC}$ = 8.1 Hz, P(CHMe_c*Me*$_d$)), 8.6 (d, J = 5.9 Hz, C_5*Me*$_5$). $^{31}P\{^1H\}$ NMR (THF-d_8): δ 33.8.

Synthesis of 4d. To a glass vial containing a magnetically stirred solution of freshly prepared **4c** (0.050 g, 0.042 mmol) in Et_2O (8 mL) was added NEt_3 (1.5 mL). The vial was then sealed with a PTFE-lined cap, and the solution was magnetically stirred for 2 h. ^{31}P NMR data collected on an aliquot of this solution indicated clean conversion to **4d**. The solvent and other volatile materials were then removed in vacuo, yielding an oily yellow solid. The solid was then washed with pentane (5 × 1.5 mL), and the product was then dried in vacuo to yield **4d** as an analytically pure pale yellow powder (0.043 g, 0.036 mmol, 85%). Anal. Calcd for $C_{51}H_{41}PNRuBF_{20}$: C 51.44; H 3.47; N 1.18. Found: C 51.21; H 3.30; N 1.13. ^1H NMR (THF-d_8): δ 5.97 (d, $^3J_{HH}$ = 6.0 Hz, 1H, C4−H or C7−H), 5.85 (d, $^3J_{HH}$ = 5.5 Hz, 1H, C7−H or C4−H), 5.55 (t, $^3J_{HH}$ = 5.5 Hz, 1H, C5−H or C6−H), 5.43 (t, $^3J_{HH}$ = 5.5 Hz, 1H, C6−H or C5−H), 3.58 (m, 1H, C1(H_a)(H_b)), 3.30 (s, 6H, NMe_2), 3.09 (m, 1H, C1(H_a)-(H_b)), 2.43 (m, 1H, P(C*H*$Me_a$$Me_b$)), 2.30 (m, 1H, P(C*H*$Me_c$$Me_d$)), 1.82 (s, 15H, C_5Me_5), 1.31 (d of d, $^3J_{PH}$ = 16.0 Hz, $^3J_{HH}$ = 7.0 Hz, 3H, P(CH*Me*$_a$$Me_b$)), 1.25 (d of d, $^3J_{PH}$ = 13.0 Hz, $^3J_{HH}$ = 7.0 Hz, 3H, P(CHMe_a*Me*$_b$)), 1.09 (d of d, $^3J_{PH}$ = 18.0 Hz, $^3J_{HH}$ = 7.0 Hz, 3H, P(CH*Me*$_c$$Me_d$)), 0.58 (d of d, $^3J_{PH}$ = 12.0 Hz, $^3J_{HH}$ = 7.0 Hz, 3H, P(CHMe_c*Me*$_d$)). $^{13}C\{^1H\}$ NMR (THF-d_8): δ 169.4 (C2), 123.1−123.0 (m, C3a and C7a), 91.7 (C_5Me_5), 87.9 (d, $^1J_{PC}$ = 31.3 Hz, C3), 83.3 (C5 or C6), 81.2 (C6 or C5), 80.2 (C4 or C7), 77.0 (C7 or C4), 41.9 (d, $^4J_{PC}$ = 16.5 Hz, NMe_2), 36.1 (d, $^3J_{PC}$ = 3.4 Hz, C1), 22.2 (P(*C*H$Me_a$$Me_b$)), 21.7 (d, $^2J_{PC}$ = 21.4 Hz, P(CH*Me*$_a$$Me_b$)), 20.4 (m, P(*C*H$Me_c$$Me_d$)), 19.8 (d, $^2J_{PC}$ = 29.9 Hz, P(CH*Me*$_c$$Me_d$)), 18.8 (d, $^2J_{PC}$ = 17.4 Hz, P(CHMe_a*Me*$_b$)), 17.2 (d, $^2J_{PC}$ = 10.8 Hz, P(CHMe_c*Me*$_d$)), 7.2 (C_5*Me*$_5$). $^{31}P\{^1H\}$ NMR (THF-d_8): δ −3.9. A crystal of **4d** suitable for single-crystal X-ray diffraction studies was grown by layering a concentrated CH_2Cl_2/diethyl ether (5:1) solution with pentane and storing the solution at −35 °C.

Synthesis of 4e. To a glass vial containing a magnetically stirred suspension of **2b** (0.11 g, 0.21 mmol) in Et_2O (5 mL) was added solid $Li(Et_2O)_{2.5}B(C_6F_5)_4$ (0.18 g, 0.21 mmol) all at once. The addition caused an immediate color change from red-orange to brown, and dissolution of **2b** occurred over the course of several minutes. The vial was then sealed with a PTFE-lined cap, and the solution was magnetically stirred for 1.5 h. After this time period, the reaction mixture was deep yellow-brown in color and a fine white precipitate had formed. ^{31}P NMR data collected on an aliquot of this crude reaction mixture solution indicated the quantitative formation of **4e**. The mixture was then filtered through Celite, yielding a clear yellow-brown solution. The reaction mixture was then concentrated in vacuo to approximately 2 mL, filtered again through Celite, and stored at −35 °C in order to induce crystallization. After 24 h, a pale yellow microcrystalline solid was isolated by transferring the supernatant solution to a new glass vial by using a Pasteur pipet; this solution was then concentrated in vacuo in order to induce further crystallization. After repeating this procedure, the isolated crops of crystals were then combined, dried in vacuo, and washed with pentane (3 × 1.5 mL) to yield **4e** as a pale yellow microcrystalline solid (0.21 g, 0.17 mmol, 83%). Anal. Calcd for $C_{51}H_{41}PNRuBF_{20}$: C 51.44; H 3.47; N 1.18. Found: C 51.64; H 3.20; N 1.49. ^1H NMR (THF-d_8): δ 7.55 (d, $^3J_{HH}$ = 7.5 Hz, 1H, C7−H), 7.44 (d, $^3J_{HH}$ = 7.0 Hz, 1H, C4−H), 7.36−7.29 (m, 2H, C5−H and C6−H), 3.84 (s, 2H, C(H_a)(H_b)), 2.85 (m, 2H, P(C*H*Me_2)$_2$), 1.98 (s, 15H, C_5Me_5), 1.25−1.18 (m, 12H, P(CH*Me*$_2$)$_2$), 0.95 (br s, 6H, NMe_2). $^{13}C\{^1H\}$ NMR (THF-d_8): δ 173.8 (d, $^2J_{PC}$ = 18.4 Hz, C2), 145.1 (d, $^3J_{PC}$ = 5.5 Hz, C7a), 138.1 (C3a), 130.8 (d, $^1J_{PC}$ = 28.9 Hz, C3), 127.3 (C5), 126.6 (C6), 125.0 (C4), 122.5 (C7), 100.3 (C_5Me_5), 51.2 (NMe_2), 34.7 (d, $^3J_{PC}$ = 9.6 Hz, C1), 25.0 (P(*C*HMe_2)$_2$), 17.8−17.6 (m, P(CH*Me*$_2$)$_2$), 10.0 (C_5*Me*$_5$). $^{31}P\{^1H\}$ NMR (THF-d_8): δ 82.3. A single crystal of **4e** grown from a concentrated diethyl ether solution at ambient temperature proved suitable for X-ray analysis.

Synthesis of 5b. To a glass vial containing a magnetically stirred suspension of **2b** (0.10 g, 0.18 mmol; **2a** can also be used, giving identical results) in benzene (5 mL) was added solid $NaN(SiMe_3)_2$ (0.034 g, 0.18 mmol) all at once. The addition caused an immediate darkening of the suspension from deep red to dark red-green. The vial was then sealed with a PTFE-lined cap, and the solution was magnetically stirred for 45 min. During this time period, the solution lightened in color from red-green to red-orange with a concomitant formation of a fine precipitate. ^{31}P NMR data collected on an aliquot of this crude reaction mixture indicated the quantitative formation of **5b**. The solution was then filtered through Celite and the benzene solvent and other volatile materials were removed in vacuo, yielding an orange solid. The solid was then washed with cold pentane (1.5 mL, precooled to −35 °C), and the product was then dried in vacuo to yield **5b** as an analytically pure bright orange powder (0.075 g, 0.15 mmol,

80%). Anal. Calcd for $C_{27}H_{40}PNRu$: C 63.50; H 7.90; N 2.74. Found: C 63.14; H 8.28; N 2.84. ^{1}H NMR (C_6D_6): δ 12.01 (br s, 1H, Ru=C−H), 7.52 (d, $^3J_{HH}$ = 8.0 Hz, 1H, C4−H), 7.35 (d, $^3J_{HH}$ = 7.5 Hz, 1H, C7−H), 7.28 (t, $^3J_{HH}$ = 7.5 Hz, 1H, C5−H), 7.10 (m, 1H, C6−H), 5.83 (s, 1H, C3−H), 4.58 (d, $^2J_{PH}$ = 13.7 Hz, 1H, C1−H), 3.06 (s, 3H, NMe), 3.00 (m, 1H, P(C*H*Me$_a$Me$_b$)), 2.02 (s, 15H, C_5Me_5), 1.51 (d of d, $^3J_{PH}$ = 15.0 Hz, $^3J_{HH}$ = 7.0 Hz, 3H, P(CH*Me*$_a$Me$_b$)), 1.28 (m, 1H, P(C*H*Me$_c$Me$_d$)), 0.91 (d of d, $^3J_{PH}$ = 15.5 Hz, $^3J_{HH}$ = 7.0 Hz, 3H, P(CHMe$_a$*Me*$_b$)), 0.78 (d of d, $^3J_{PH}$ = 14.5 Hz, $^3J_{HH}$ = 7.5 Hz, 3H, P(CH*Me*$_c$Me$_d$)), 0.49 (d of d, $^3J_{PH}$ = 11.0 Hz, $^3J_{HH}$ = 7.5 Hz, 3H, P(CHMe$_c$*Me*$_d$)), −11.80 (d, $^2J_{PH}$ = 38.5 Hz, 1H, Ru−H). ^{13}C{^{1}H} (C_6D_6): δ 240.6 (Ru=*C*H), 153.8 (C2), 144.5 (C3a), 139.0 (C7a), 126.7 (C5), 124.4 (C4), 121.9 (C6), 119.6 (C7), 104.8 (C3), 95.6 (*C*$_5$Me$_5$), 51.6 (C1), 48.0 (NMe), 28.8 (P(*C*HMe$_c$Me$_d$)), 24.7 (P(*C*HMe$_a$Me$_b$)), 19.8 (P(CH*Me*$_a$Me$_b$)), 19.2 (P(CH*Me*$_c$Me$_d$)), 18.2 (P(CHMe$_c$*Me*$_d$)), 17.3 (P(CHMe$_a$*Me*$_b$)), 11.7 (C_5*Me*$_5$). ^{31}P{^{1}H} NMR (C_6D_6): δ 112.6.

Synthesis of 5c. To a glass vial containing a magnetically stirred suspension of **2b** (0.24 g, 0.44 mmol; **2a** can also be used giving identical results) in toluene (8 mL) was added solid NaN(SiMe$_3$)$_2$ (0.081 g, 0.44 mmol) all at once. The addition caused an immediate darkening of the suspension from deep red to a green-red mixture. The vial was then sealed with a PTFE-lined cap, and the solution was magnetically stirred for 24 h. During this time period, the solution lightened in color from green-brown to red-orange with a concomitant formation of a fine precipitate. ^{31}P NMR data collected on an aliquot of this crude reaction mixture indicated the quantitative formation of **5c**. The solution was then filtered through Celite, and the toluene solvent and other volatile materials were removed in vacuo, yielding an orange solid. The solid was then washed with cold pentane (1.5 mL, precooled to −35 °C), and the product was then dried in vacuo to yield **5c** as an analytically pure bright orange powder (0.19 g, 0.37 mmol, 84%). Anal. Calcd for $C_{27}H_{40}PNRu$: C 63.50; H 7.90; N 2.74. Found: C 63.48; H 7.88; N 2.88. ^{1}H NMR (C_6D_6): δ 12.09 (br s, 1H, Ru=C−H), 7.76 (d, $^3J_{HH}$ = 8.0 Hz, 1H, C4−H or C7−H), 7.28 (t, $^3J_{HH}$ = 7.5 Hz, 1H, C5−H or C6−H), 7.18 (m, 1H, aryl-H), 7.12 (m, 1H, aryl-H), 3.09 (br m, 1H, P(C*H*Me$_a$Me$_b$)), 2.95−2.71 (m, 5H, NMe and C(H_a)(H_b)), 2.20−1.93 (m, 16H, C_5Me_5 and P(C*H*Me$_c$Me$_d$)), 1.32 (m, 3H, P(CH*Me*$_a$Me$_b$)), 1.13 (m, 3H, P(CHMe$_a$*Me*$_b$)), 1.07−0.95 (m, 6H, P(CH*Me*$_c$Me$_d$)), −12.38 (d, $^2J_{PH}$ = 46.5 Hz, 1H, Ru−H). ^{13}C{^{1}H} NMR (C_6D_6): δ 244.1 (d, $^2J_{PC}$ = 17.4 Hz, Ru=*C*H), 158.3 (d, $^2J_{PC}$ = 10.8 Hz, C2), 147.8 (C7a), 136.9 (d, $^2J_{PC}$ = 6.4 Hz, C3a), 126.9 (C5 or C6), 123.1 (aryl-*C*H), 122.3 (aryl-*C*H), 121.4 (C4 or C7), 105.8 (d, $^1J_{PC}$ = 40.6 Hz, C3), 96.9 (*C*$_5$Me$_5$), 47.8 (NMe), 40.5 (d, $^3J_{PC}$ = 6.0 Hz, C1), 32.1 (d, $^1J_{PC}$ = 17.4 Hz, P(*C*HMe$_a$Me$_b$)), 26.0 (d, $^1J_{PC}$ = 35.0 Hz, P(*C*HMe$_c$Me$_d$)), 20.6 (P(CH*Me*$_a$Me$_b$)), 20.1 (P(CH*Me*$_c$Me$_d$) or (P(CHMe$_c$*Me*$_d$)), 19.4−19.3 (m, P(CHMe$_a$*Me*$_b$) and either (P(CH*Me*$_c$Me$_d$) or (P(CHMe$_c$*Me*$_d$)), 11.9 (C_5*Me*$_5$). ^{31}P{^{1}H} NMR (C_6D_6): δ 78.2. Slow evaporation of a diethyl ether/toluene (5:1) solution of **5c** produced a crystal suitable for single-crystal X-ray diffraction analysis.

Synthesis of 5a·CH$_3$CN. To a glass vial containing a magnetically stirred orange solution of **2b** (0.20 g, 0.37 mmol) in MeCN (7 mL) was added solid anhydrous K_2CO_3 (0.10 g, 0.73 mmol) all at once. The vial was then sealed with a PTFE-lined cap, and the solution was magnetically stirred for 48 h. During this time period, the reaction mixture gradually lightened from an orange suspension into a yellow-orange suspension. The reaction mixture was filtered through Celite to yield a yellow-orange solution, and ^{31}P NMR data collected on an aliquot of this crude reaction mixture indicated the quantitative formation of **5a**·CH$_3$CN. The MeCN solution was stored at −35 °C in order to induce crystallization. After 24 h, crystals of **5a**·CH$_3$CN were isolated by transferring the supernatant solution to a new glass vial by using a Pasteur pipet; this solution was then concentrated in vacuo in order to induce further crystallization. After repeating this procedure, the isolated crops of crystals were then combined and dried in vacuo, yielding **5a**·CH$_3$CN as an analytically pure yellow-orange crystalline solid (0.17 g, 0.30 mmol, 83%). Anal. Calcd for $C_{29}H_{43}PN_2Ru$: C 63.13; H 7.86; N 5.08. Found: C 62.91; H 7.84; N 5.33. Whereas the ^{1}H NMR spectrum of **5a**·CH$_3$CN in CD$_3$CN at 300 K exhibited broadened resonances due to rapid exchange between free and bound acetonitrile molecules, sharp ^{1}H and ^{13}C NMR signals were observed at 273 K. ^{1}H NMR (CD$_3$CN, 273 K): δ 7.28 (d, $^3J_{HH}$ = 7.5 Hz, 1H, C4−H), 7.02 (d, $^3J_{HH}$ = 7.5 Hz, 1H, C7−H), 6.43−6.37 (m, 2H, C5−H and C6−H), 5.77 (d, $^4J_{PH}$ = 4.0 Hz, 1H, C1−H), 3.36 (m, 1H, P(C*H*Me$_a$Me$_b$)), 3.06 (s, 3H, NMe$_a$), 3.00 (s, 3H, NMe$_b$), 2.39 (m, 1H, P(C*H*Me$_c$Me$_d$)), 1.54 (s, 15 H, C_5Me_5), 1.33 (d of d, $^3J_{PH}$ = 9.5 Hz, $^3J_{HH}$ = 7.5 Hz, 3H, P(CH*Me*$_c$Me$_d$)), 1.21 (d of d, $^3J_{PH}$ = 15.5 Hz, $^3J_{HH}$ = 6.5 Hz, 3H, P(CH*Me*$_a$Me$_b$)), 0.92 (d of d, $^3J_{PH}$ = 17.0 Hz, $^3J_{HH}$ = 7.0 Hz, 3H, P(CHMe$_c$*Me*$_d$)), 0.67 (d of d, $^3J_{PH}$ = 14.0 Hz, $^3J_{HH}$ = 7.0 Hz, 3H, P(CHMe$_a$*Me*$_b$)). ^{13}C{^{1}H} (CD$_3$CN, 273 K): δ 164.1 (d, $^2J_{PC}$ = 24.7 Hz, C2), 135.9 (d, $^2J_{PC}$ = 8.6 Hz, C3a), 128.2 (C7a), 118.9 (C4), 118.7 (C7), 113.8 (C5 or C6), 113.7 (C6 or C5), 85.5 (d, $^1J_{PC}$ = 49.3 Hz, C3), 85.0 (d, $^3J_{PC}$ = 10.1, C1), 82.3 (*C*$_5$Me$_5$), 63.4 (NMe$_a$), 53.8 (NMe$_b$), 26.8 (m, P(*C*HMe$_c$Me$_d$)), 24.8 (m, P(*C*HMe$_a$Me$_b$)), 21.1 (P(CHMe$_c$*Me*$_d$)), 19.4 (P(CHMe$_a$*Me*$_b$)), 19.1 (P(CH*Me*$_c$Me$_d$)), 18.4 (P(CH*Me*$_a$Me$_b$)), 9.8 (C_5*Me*$_5$). ^{31}P{^{1}H} NMR (CD$_3$CN, 273 K): δ 44.3. A crystal of (**5a**·CH$_3$CN)·0.5CH$_3$CN suitable for single-crystal X-ray diffraction studies was grown from a concentrated MeCN solution at ambient temperature.

Synthesis of 6. Diphenylphosphine (35 μL, 0.20 mmol) was added all at once to a glass vial containing a magnetically stirred solution of **5c** (0.10 g, 0.20 mmol) in toluene (4 mL). The vial was then sealed with a PTFE-lined cap, and the solution was magnetically stirred for 3 h. During this time period, the solution gradually lightened in color from deep orange to yellow. ^{31}P NMR data collected on an aliquot of this solution indicated the quantitative formation of **6**. The solvent and other volatile materials were removed in vacuo, and the residue was taken up in a minimal amount of pentane (approximately 5 mL) and subsequently filtered through Celite. The pentane solution was stored at −35 °C in order to induce crystallization. After 24 h, crystals of **6** were isolated by transferring the supernatant solution to a new glass vial by using a Pasteur pipet; this solution was then concentrated in vacuo in order to induce further crystallization. After repeating this procedure, the isolated crops of crystals were then combined and dried in vacuo, yielding **6** as an analytically pure yellow microcrystalline solid (0.097 g, 0.14 mmol, 70%). Anal. Calcd for $C_{39}H_{51}P_2NRu$: C 67.22; H 7.38; N 2.01. Found: C 67.47; H 7.39; N 2.16. ^{1}H NMR (C_6D_6): δ 7.55−7.52 (m, 3H, aryl-Hs), 7.28 (t, $^3J_{HH}$ = 8.0 Hz, 1H, C5−H or C6−H), 7.23 (d, $^3J_{HH}$ = 7.0 Hz, 1H, C4−H or C7−H), 7.18−7.01 (m, 8H, aryl-H's), 6.98 (d, $^3J_{HH}$ = 7.0 Hz, 1H, C6−H or C5−H), 6.44 (d of d, $^1J_{PH}$ = 340.1 Hz, $^3J_{PH}$ = 12.0 Hz, 1H, P*H*Ph$_2$), 3.72 (m, 1H, N−C(H_a)(H_b)−Ru), 3.46 (m, 1H, P(C*H*Me$_a$Me$_b$)), 3.17−3.04 (m, 2H, C(H_c)(H_d)), 2.76 (m, 1H, N−C(H_a)(H_b)−Ru), 2.20 (m, 1H, P(C*H*Me$_c$Me$_d$)), 1.93 (s, 3H, NMe), 1.64 (s, 15 H, C_5Me_5), 1.39 (d of d, $^3J_{PH}$ = 10.0 Hz, $^3J_{HH}$ = 7.0 Hz, 3H, P(CH*Me*$_c$Me$_d$)), 1.33 (d of d, $^3J_{PH}$ = 17.0 Hz, $^3J_{HH}$ = 7.0 Hz, 3H, P(CH*Me*$_a$Me$_b$)), 1.13−1.08 (m, 6H, P(CHMe$_a$*Me*$_b$) and P(CHMe$_c$*Me*$_d$)). ^{13}C{^{1}H} NMR (C_6D_6): δ 167.0 (d, $^2J_{PC}$ = 12.0 Hz, C2), 152.0 (aryl-C), 137.3−137.0 (m, aryl-C's), 135.7 (d, J_{PC} = 7.0 Hz, aryl−C), 134.7 (d, J_{PC} = 11.3 Hz, aryl−*C*H), 133.0 (d, J_{PC} = 9.1 Hz, aryl−*C*H), 127.0 (aryl−*C*H), 126.9 (d, J_{PC} = 3.6 Hz, aryl−*C*H), 122.2 (C4 or C7), 119.0 (aryl−*C*H), 118.5 (C5 or C6), 90.9 (*C*$_5$Me$_5$), 86.5 (d, $^1J_{PC}$ = 41.9 Hz, C3), 45.1 (NMe), 43.7 (m, NCH$_2$), 41.0 (d, $^3J_{PC}$ = 6.9 Hz, C1), 31.7 (P(*C*HMe$_c$Me$_d$)), 26.2 (d, $^1J_{PC}$ = 27.3 Hz, (P(*C*HMe$_a$Me$_b$)), 21.5 (d, $^2J_{PC}$ = 7.3 Hz, P(CH*Me*$_c$Me$_d$)), 20.3 (P(CHMe$_a$*Me*$_b$) or (P(CHMe$_c$*Me*$_d$)), 19.3−19.2 (m, P(CH*Me*$_a$Me$_b$) and either (P(CHMe$_a$*Me*$_b$) or (P(CHMe$_c$*Me*$_d$)), 10.4 (C_5*Me*$_5$). ^{31}P{^{1}H} NMR (C_6D_6): δ 54.2 (d, $^2J_{PP}$ = 38.5 Hz), 45.1 (d, $^2J_{PP}$ = 38.5 Hz). A

crystal of **6**·0.5C_5H_{12} suitable for X-ray diffraction analysis was grown from pentane at −35 °C.

Crystallographic Solution and Refinement Details. All crystallographic data were obtained at 193(±2) K on a Bruker PLATFORM/SMART 1000 CCD diffractometer using graphite-monochromated Mo Kα ($\lambda = 0.71073$ Å) radiation, employing samples that were mounted in inert oil and transferred to a cold gas stream on the diffractometer. The structures were solved either by use of a Patterson search/structure expansion (for **2a** and (**5a**·CH_3CN)·0.5CH_3CN) or by use of direct methods, and refined by use of full-matrix least-squares procedures (on F^2) with R_1 based on $F_o^2 \geq 2\sigma(F_o^2)$ and wR_2 based on $F_o^2 \geq -3\sigma(F_o^2)$. In the case of **2a**, the crystal used for data collection was found to display nonmerohedral twinning. As a result, the structural refinement of **2a** was carried out by employing a disorder model featuring two independent molecules of **2a** refined with an occupancy factor of 0.5, in which only the Ru, Cl, P, and N atoms were refined anisotropically; full refinement details are provided in the Supporting Information. A positional disorder involving a portion of one of the isopropyl fragments that was noted during the refinement of **5c** was satisfactorily treated by employing an 80 (C24A and C26A, refined anisotropically):20 (C24B and C26B, refined isotropically) disorder model; only the major component is shown. With the exception of the disordered atoms noted above and the disordered pentane solvates in **3b**·1.5C_5H_{12} and **6**·0.5C_5H_{12}, anisotropic displacement parameters were employed throughout for the non-hydrogen atoms. With the exception of the Ru-*H*'s in **4e** and **5c** (the positions of which were located in the difference map and refined) all H atoms were added at calculated positions and refined by use of a riding model employing isotropic displacement parameters based on the isotropic displacement parameter of the attached atom. For complete experimental details and tabulated crystallographic data, see the Supporting Information.

Acknowledgment is made to the Natural Sciences and Engineering Research Council (NSERC) of Canada (including a Discovery Grant for M.S. and a Postgraduate Scholarship for M.A.R.), the Killam Trust (Dalhousie University; including a Research Prize for M.S. and a Predoctoral Scholarship for M.A.R.), the Canada Foundation for Innovation, the Nova Scotia Research and Innovation Trust Fund, and Dalhousie University for their generous support of this work. We also thank Drs. Bob Berno and Michael Lumsden (Atlantic Region Magnetic Resonance Center, Dalhousie) for assistance in the acquisition of NMR data.

Note Added in Proof. A closely related double geminal C−H bond activation process has recently been reported: Ingleson, M. J.; Yang, X.; Pink, M.; Caulton, K. G. *J. Am. Chem. Soc.* **2005**, *127*, 10846.

Supporting Information Available: Tabulated single-crystal X-ray diffraction data for **2a**, **2b**, **3a**, **3b**·1.5C_5H_{12}, **4d**, **4e**, (**5a**·CH_3CN)·0.5CH_3CN, **5c**, and **6**·0.5C_5H_{12}, as well as ^1H and $^{13}C\{^1H\}$ NMR spectra for **4e** (obtained at 300 K) are available free of charge via the Internet at http://pubs.acs.org.

OM050534E